Development of an algorithm for estimating Lead-Acid Battery State of Charge and State of Health.

Mateusz Michal Samolyk

Jakub Sobczak

This thesis is presented as part of Degree of

Master of Science in Electrical Engineering

Blekinge Institute of Technology

September 2013

Blekinge Institute of Technology

School of Engineering

Department of Electrical Engineering

Supervisor: Sen. Lec. Anders Hultgren

Examiner: Dr. Sven Johansson

Abstract – **In this paper, a state of charge (SOC) and a state of health (SOH) estimation method for lead-acid batteries are presented. In the algorithm the measurements of battery's terminal voltage, current and temperature are used in the process of SOC calculation. The thesis was written in cooperation with Micropower AB. The algorithm was designed to fulfill the specific requirements of the electric vehicles application: an error below 5% of SOC, computational simplicity and the possibility of being implemented in a basic programming languages. The current used method at Micropower, Coulomb counting, is compared with a method presented by Chiasson and Vairamohan 2005 based on modified Thevein circuit during charging and discharging of the battery. The Thevenin based method gave better result compared to Coulomb counting but seems not to fulfill Micropowers requirements. A correction method based on periods of no charging or discharging, possible to be used together with Coulomb counting as well as with the Thevenin method was developed. The evaluation method indicates that when using also the correction method the Micropowers requirements are fulfilled.**

Keywords: : Lead-Acid Battery, SOC, SOH, Improved Coulomb Counting

Acknowledgments

We would like to thank our supervisor, Prof. Anders Hultgren for his time and support he has provided us with during writing this thesis, Henrik Magnusson and the rest of the Micropower AB staff for their advices and granting us the necessary equipment.

Table of Contents

1. Introduction

Electricity plays a crucial role in everyone's life nowadays. It is used in a variety of different devices with people accustomed to them too much to even notice how necessary they became. However, with the tremendous technological progress in electronic industry many challenges arise. Even though the Devices' performance is growing exponentially their size is constantly minimized in order to satisfy the modern customer needs.

A decade ago mobility used to be a synonym of freedom, nowadays mobility is a standard. With mobility being a requirement of electronic devices, there comes another one - a need of a reliable mobile energy storage - a Battery. A battery for an Electric Vehicle is equivalent to the fuel tank for a typical, gasoline car. Imagine a car without the fuel-level indicator on the dashboard. Notice how inconvenient would it be for the driver not to have the precise indicator of how many miles the car can still travel.

With the popularization of the Electric Vehicles and Hybrid-Electric Vehicles, such as cars, forklifts and the wheelchairs there is a growing demand for a Battery State of Charge indicator, a software or hardware designed to estimate the remaining effective capacity of the battery having only the measurements of limited number of variables.

The aim of this paper is to cover the Lead-Acid battery State of Charge and State of Health estimation problem and produce a viable solution in the form of algorithm, capable of estimating those two states with a minimal input required from the operator.

The introduction to the topic and the theoretical background is included in the first two chapters of this Thesis. The third one covers the project requirements, practical description of the algorithm, its implementation and the laboratory setup. The fourth chapter includes the data from the tests carried out in the laboratory and its comparison with the reference data as well. The fifth one concludes the research and contains suggestions towards a future work in the area of Battery State of Charge and State of Health estimation. The references are grouped and described in the last chapter of this paper.

2. Theoretical Background

2.1. Lead-Acid batteries

2.1.1. Lead-Acid Battery structure, the principle of its operation

There are two main battery system categories, i.e.:

1. Batteries which convert their chemical energy into electrical only once (primary cells)
2. Batteries which can convert chemical energy into electrical multiple times (secondary cells)

The second type of batteries are much more practical than the primary type, as their usage is by far more cost-efficient as it allows for long terms of use.

The basic battery structure is presented in the figure 2.1.1. It consists of two electrodes, the negative and positive one connected to the two terminals leading outside of the battery. The electrodes are immersed in the electrolyte which separates them and also participates in the chemical reactions taking place inside the battery. Through the flow of electrons from the negative to positive electrodes the current is formed which can be drawn from the battery.

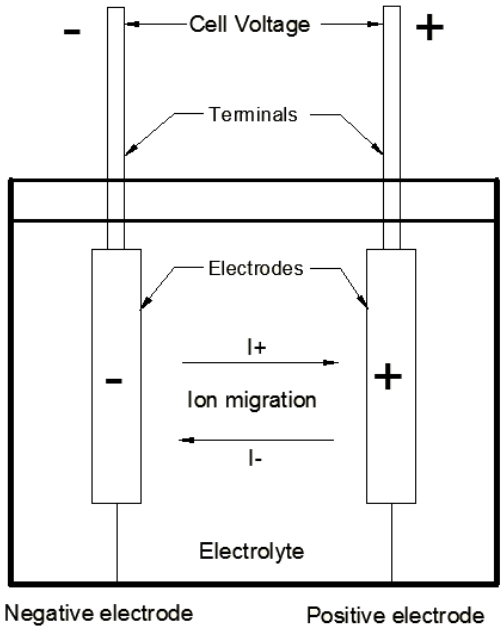

Fig. 2.1.1 Electrochemical cell [12]

The basic battery structure is suited for both types of batteries. A battery is characterized by the chemical reaction taking place inside of it, the cell reaction. In order to properly explain the battery operation a closer look must be taken into the cell reaction of the battery [12]. Fully charged battery contains only high energy chemical compounds, which are converted into lower energy compounds during the process of discharging. Similarly, when the battery is charged the reaction is reversed, requiring sufficient amount of energy to be supplied to the cell. In the batteries, the cell reaction is divided into two separate electrode reactions by design in order to ensure that the released energy takes form of electrical energy instead of heat. The current is created by the flow of electrons between two electrodes. The cell reaction for the battery is as follows[12]:

$$S(N)_{red} + S(P)_{ox} \Rightarrow S(N)_{ox} + S(P)_{red} + energy \quad (1)$$

Where:

$$S(N)_{red} \Rightarrow S(N)_{ox} + n * e \quad (2)$$

$$S(P)_{ox} + n * e \Rightarrow S(P)_{red} \quad (3)$$

S(N) – negative substance

S(P) – positive substance

$S(P)_{ox}$– oxidized

red – reduced

During the process of discharging the battery, according to the presented chemical reactions, the substance in the negative electrode is oxidized by the oxidizing substance. It is located in the positive electrode and is reduced as a result of the process. The energy that can be drawn from the cell is represented by the difference of chemically bonded energy between the starting and the final composition of the cell reaction (1). However, it must be noted that part of the energy is lost as a heat in the process.

2.1.2. Electric model of the battery

In order to give better understanding of the operation of batteries, electrical network of the battery is introduced by using typical electrical components. This process is of great help for an electric engineer to analyze the behavior of the battery, as it’s based on his primary

knowledge. Battery is an electric bipole, so it could be represented simply by electromotive force and an internal impedance, if it were linear. However, the battery is nonlinear, meaning that both the electromotive force and impedance are functions of the battery state of charge. Electrical model which takes into account the nonlinearity of the battery as well as the fact that its charge efficiency will not be perfect is presented in figure 2.1.2. :

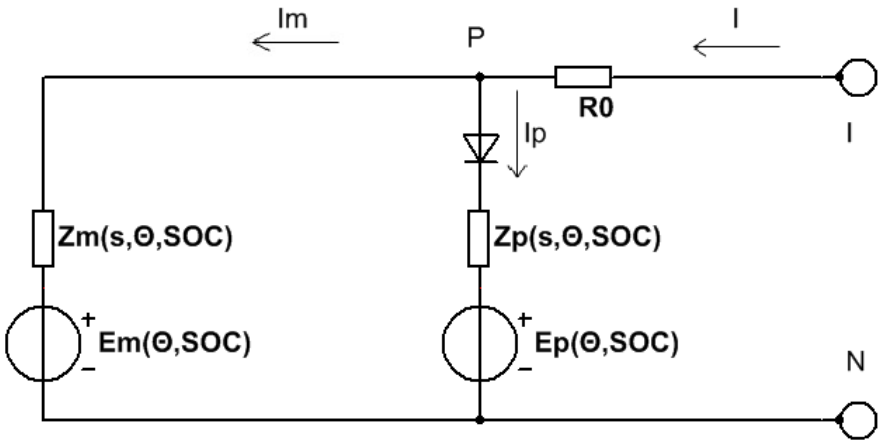

Fig. 2.1.2 Electric model of a general battery considering the parasitic reaction [3]

Firstly, it should be noted that the elements Z and E are function of the battery state of charge (SOC) and the electrolyte temperature (Θ). It can be observed that only some part (I_m) of the total current (I) take part in the main reaction. The p branch represents the parasitic reactions present in the battery, energy in the p branch is converted into other forms of energy. In the case of the lead-acid batteries the energy is absorbed through the water dissociation reaction, which is the separation of oxygen and hydrogen. Dissipation of the thermal power in the impedances Z_m and $Z_p$is the source of heating of the battery.

With the addition of a priori knowledge, the conditions for inactiveness of the parasitic branch, the model presented in figure 2.1.2 can be simplified, representing a specific type of battery. The electrical model for the lead-acid battery is presented in the figure 2.1.3. In the case of lead-acid batteries, their charge efficiency is very close to unity while the voltage is below a threshold level on the battery [3]. The model is divided into two branches, the parasitic and the main reaction branch represented by $_p$ and $_m$ indexes respectively.

The identification of the main branch can be done by observation of the battery step responses, the input can be set as step current from the constant value of I to 0, the observed output is the battery's voltage. With the assumption that the parasitic branch is inactive, meaning it draws no current, the identification will be simpler. The measurement of the battery step responses is done at different SOC and electrolyte temperature values. The

process of identification in this case is very complex and highly dependent on the number of R-C blocks. Moreover, the model parameters change at different paces depending on the environment they are used in.

The parasitic branch is less complex. Experimental work has proven that [3] internal impedance Z_p could be modeled as a simple resistor. However, the model cannot be designed as linear since there is a nonlinearity in the relation of the current I_p with the voltage at parasitic branch terminals V_{PN}.

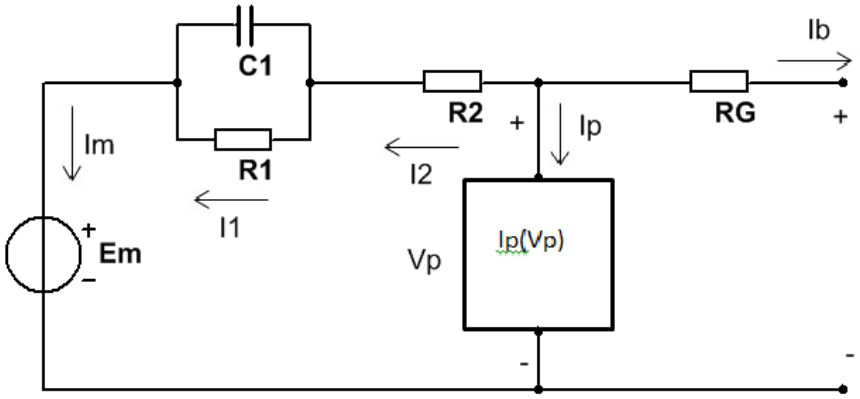

Figure 2.1.3 The electric network model for lead-acid batteries [3]

In the figure 2.1.3 the resistor R_2 is a function of the state of charge of the battery (SOC). The presented model requires a choice of reference current I^*. The choice of reference current as well as all of the necessary equations are shown in detail in [3]. The capacitance is dependent on the electrolyte freezing temperature and empirical coefficients which are constant for a given battery and chosen reference current.

2.1.3. Lead-Acid battery types

The lead-acid batteries can be subdivided into the three categories, in accordance to technology used in the battery construction, i.e:

- Vented/wet cell (flooded) batteries
- Absorbed Glass Mat (AGM) batteries
- Gel cell batteries

Vented/wet cell (flooded) batteries

Flooded batteries are the most commonly used lead-acid batteries nowadays. Due to their relatively low prices (compared to the gel and AGM batteries), many size options and versatility, they have found their application in a variety of industrial branches. The term "flooded" is used to indicate the excess of electrolyte fluid, in which the plates are completely submerged [17]. The use of wet cell batteries has many advantages. Not only the flooded lead-acid batteries can be easily maintained by adding distilled water, but also their operations are much more stable in high temperatures (>32° C) compared to the other types. Moreover they are widely available and have a long history of use, which in some way proves their high reliability and usefulness. On the other hand these kind of batteries may be used only in upright position. They produce oxygen and hydrogen when charging, and then require constant ventilation. It may produce hazardous acid spray if it gets drastically overcharged and has a higher discharge rate than the other types of Lead-Acid Batteries. This type of the battery will be used during the project presented in this paper.

AGM (Absorbed Glass Mat) batteries

AGM is one of the types of VLRA (valve regulated lead acid battery). In this system fiber separators are introduced to prevent the leakage of acid. It is achieved through absorption of the liquid electrolyte [12], while allowing a number of the pores to be empty. Those unfilled pores are channels, through which the oxygen can migrate from the positive to negative plates. The glass mat absorption property is crucial in the process as it allows high compression of the gel and a narrow contact may be maintained between the plates and the separator [17]. The separator should not be saturated with liquid, in order to keep the pores free for the oxygen migration. AGM batteries have numerous advantages, i.e. they are less expensive than Gel batteries, have slowest self-discharge from all of the types, best shock/vibration resistance and much wider temperature range than Gel or Flooded batteries [17]. However, the initial capacity is slightly lower than the capacity of vented batteries (around 80% of the comparable flooded battery [12]).

Gel Cell batteries

Although the gel cell battery bases on oxygen recombination, the method to achieve it slightly differs. This kind of batteries is filled with a thixotropic gel of silica mixed with sulphuric acid [17]. All of the space in the battery is filled with it, forming a solid matrix. In the beginning of a battery life time it behaves exactly like the flooded type as all of the separator's pores are filled and there are no oxygen channels at all. With time the gel dries out, shrinks and forms a numerous cracks, creating the oxygen channels, which allows the oxygen to migrate to negative plate and therefore be recombined. The gel batteries perform better than AGM batteries in two cases, in low power applications and when the regular deep discharge is required [17]. There are several drawbacks of the gel batteries as well, e.g. they are more expensive than other types, have much higher self-discharge rate than AGM batteries and are less operational at low temperatures (<40 degrees F).

2.1.4. Lead-acid batteries applications

Lead-acid batteries are a significant part in everyone's everyday life. They serve as a starter battery for vehicles - cars, buses, electric forklifts, wheelchairs, public transportation and boats. They are the main emergency power supply for different electrical systems, ensuring that the most important devices are operational and no data is lost during the blackout situations. The lead-acid batteries are crucial for telecommunication companies as they enable back-up supply during the cataclysms and power outages [18]. The three main types of lead-acid batteries (i.e. flooded, AGM and gel) have found their specific applications, e.g. the valve-regulated batteries are preferred in the systems that require high deep discharge ability and the maintenance cannot be undertaken (maintenance-free VRLA batteries). Furthermore the VLRA batteries are operational in horizontal position and do not require ventilation, what may save a lot of space, which is a crucial feature in battery rooms.

2.2. Other popular battery types and their applications

Apart from the lead-acid batteries there are four most commonly used battery types: lithium-ion, lithium-air, nickel-cadmium and silver-oxide batteries, which applications will be described briefly as this project is focused on lead-acid batteries.

Lithium-ion (Li-Ion) battery is more stable version of its predecessor - lithium metal battery. Li-ion battery finds its application both in easily recharged devices, such as cell phones and in systems, in which recharging is difficult or impossible, e.g. cardiac peacemakers. It can handle large number of recharges, without losing much capacity, making it a perfect battery for portable electronic devices. Li-ion batteries are useful in the medical application, i.e. as a battery for implantable electronic devices - pacemakers, defibrillators, neurostimulators etc. as they are small, reliable and able to last for years [12].

Lithium-air battery - another lithium-based battery, introduced in early 1990s, is still in the stage of development. This type of battery is expected to replace the lithium-ion batteries, as its energy density is potentially five to fifteen times larger [1]. Currently most of the li-air battery applications concern the automotive industry as weight is a primary concern there.

Nickel-cadmium (Ni-Cd) battery is a standard for second type of batteries. Being very durable and scalable they are often used in a variety of industrial machines, such as a portable machinery or heavy duty tools, when other sources of power are not available. Due to their ability to work in a harsh environmental conditions, they make perfect batteries for the machines vulnerable to dust and dirt, such as portable drills, portable communication tools, like two way radios (walkie-talkie type) and other field equipment [12].

Silver-Oxide batteries are known for their long operating life. The small silver-oxide batteries are relatively cheap and have many advantages over other types of cells. Their operating voltage is higher than mercury batteries. Silver-Oxide batteries are capable of providing nearly instant high power even after prolonged use in high temperature environment [8].

2.3. Battery variables

There are a number of variables which need to be known in order to build a proper model of a battery. The list of the most important ones will be presented below:

Voltage

There are two methods of deriving the voltage of a battery, depending on the reversibility of the system. Cell voltage can easily be derived from the thermodynamic data, if the system is reversible [12].

The equation representing the reaction from which the equilibrium voltage can be derived is as follows :

$$U = \frac{\Delta G}{n * F}$$

Where:

ΔG = free enthalpy of reaction, the maximum amount of chemical energy that can be converted into electrical energy and vice versa

n = number of exchanged electronic charges

F = Faraday constant

It is necessary to distinguish the difference between the open circuit voltage (OCV) and the closed circuit voltage (CCV). Most of the systems are not reversible and thus require the measurement of OCV, which can also be used as a mean to determine the SOC of the battery. Deriving closed circuit voltage (CCV) is much harder, due to its dependence on the current, SOC and the history of the cell [12].

Capacity

Capacity of the battery is defined as a number of electrical charges in Ah units which can be drawn from the battery. This parameter decreases steadily with the aging of the battery. Proper estimation of the change of battery's parameters is imperative for long term use of the battery. Precise estimation of the capacity is dependent on many variables, most significantly:

- Design of the battery
- Discharge current
- Temperature

Moreover, the important variable with regard to both capacity and the state of health (SOH) is the depth of discharge (DOD). In case of lead-acid batteries, deep discharges below the maximum value of DOD can rapidly decrease its service life [12].

Internal resistance

Internal resistance is used in order to measure the capability of the battery to handle a load, as well as to determine its power output. The general rule concerning DC resistance is

that it must be significantly lower than that of the load. However, it must be noted that the term does not represent simple ohmic resistance, as it depends on the operational conditions as well as the SOC of the battery. The internal resistance can be calculated using the direct-current method:

$$R_i = \frac{U_1 - U_2}{i_2 - i_1} = \frac{\Delta U}{\Delta i}$$

Direct-current method compares the voltage at two different loads. The current i_1 acts as the first load, resulting in appearance of voltage U_1. Afterwards, the current is increased to the value of i_2 leading to decrease in voltage up to the value of U_2.

Deriving the AC internal resistance of battery is a complex procedure, as the AC characteristics of the battery cannot be obtained directly, but through approximation of an equivalent circuit. This issue will not be explained in the paper.

Self-discharge

Self-discharge parameter represents the losses of charge in the electrodes while the battery is in open circuit. There are many reasons for the self-discharge, few of which are listed below [12]:

- Gradual reduction of the oxidation state in the positive electrode
- Mixed potentials in the secondary reactions
- Oxidizable or reducible substances in the electrolyte

There are also several processes which are misinterpreted as self-discharge, ex. increase in the internal resistance that happens after prolonged storage of primary cells, and causes a reduction in delivered capacity.

2.4. Lead-Acid battery aging process

Due to the nature of lead-acid batteries operation, which is based on conversion from the chemical energy into electrical one, several major aging processes occur [11]:

- Anodic corrosion
- Positive mass degradation
- Irreversible formation of lead sulfate in the active mass
- Short circuits
- Loss of water

Important term when considering the aging process of a battery is its state of health (SOH). It is used as indicator of the performance of the battery both in the state of charge and discharge, it may also contain information concerning the degradation of the battery. In order to design a method to predict the lifetime of the battery major ageing processes must be taken into account as well as the interaction between them [13]. Developing proper tests to analyze the complex interactions and linking them to the lifetime expectancy has proven to be great challenge. It has been proven that differentiating the effects of single ageing process can be possible only up to a certain level [13].

2.5. State of charge monitoring methods for lead acid batteries

As mentioned in the last chapter, lead acid batteries are used in numerous applications, which require high reliability, robustness and predictability. The reliable state of charge estimation strategy is a necessity in such uses as hybrid vehicles, electric vehicles and telecommunications power supplies, therefore several ways of SOC estimation are widely known in the industry. Accurate method of the SOC estimation may prevent the battery from getting deeply discharged or frequently overcharged, both of which greatly reduce the battery remaining life. Before the methods will be presented, it is important to state the SOC estimation accuracy, which is demanded for the different battery applications.

In Hybrid Electric Vehicles (HEV) the battery acts as a starter for the motor so any imprecise SOC readings with an error over 5% can seriously affect the engine's fuel efficiency and the motor operations. For the following reason in HEV applications the SOC estimation must be as precise as possible with an error's value never exceeding the 5% of the capacity measurement [16].

However, in Electric Vehicles (EV) the battery SOC determines the distance the vehicle is able to cover. The battery SOC in electric vehicles resembles the fuel tank from traditional vehicles, which are notoriously imprecise (usually about 5% measurement error) so

the borderline of 5%-7% errors in the EV applications could possibly be acceptable. During the process of designing the SOC estimation method for EV it is important not to mistake the state of charge with the capacity of a battery. Those two are usually mistaken because of their equality in the beginning of the battery use, however they begins to differ with the decrease in the battery state of health. SOC estimation is highly dependent on the battery aging process and after a certain number of charging/discharging cycles 20% or bigger error may occur [16]. For that reason state of charge of a battery should estimate the energy content and the power capability of a battery.

2.5.1. Open circuit voltage method

The OCV method uses the voltage of a battery cell as an indicator of a current battery SOC. The SOC of a battery as a semi-linear function of the open circuit voltage as presented in the figure 2.5.1. Although the open circuit voltage method is known as an accurate indicator of the SOC, this method cannot be regarded as a real-time monitoring strategy as the voltage readings take much time to stabilize. The OCV stabilization example is shown in the figure 2.5.2. Results of this method can vary depending on the measurement conditions, ex. actual voltage level, temperature, discharge rate and the age of the cell [6].

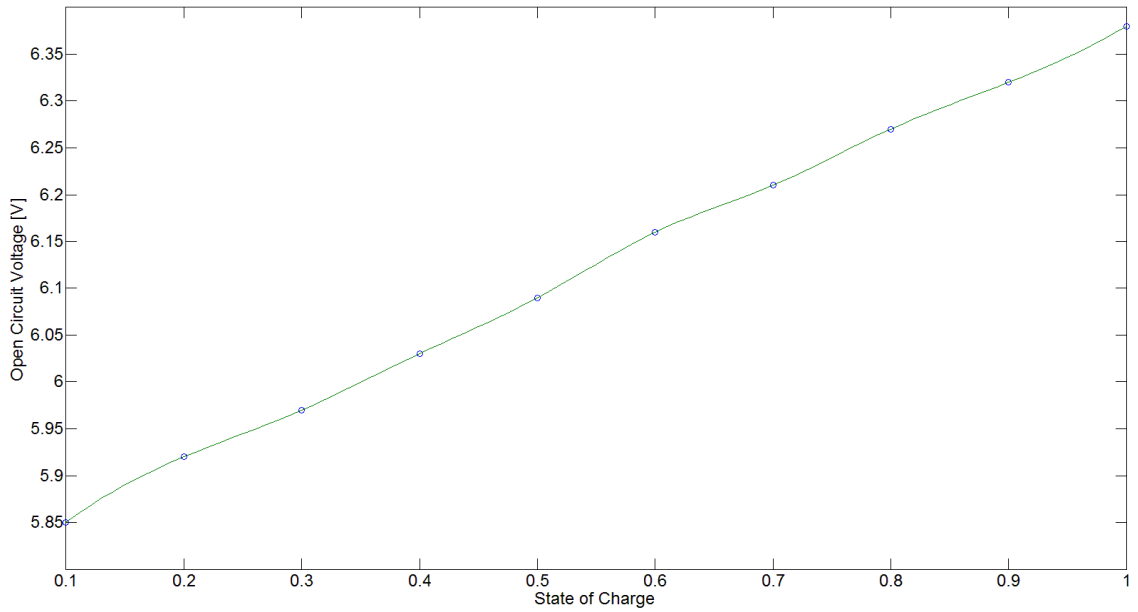

Fig. 2.5.1 The open circuit voltage to residual capacity relation of lead acid battery experiment.

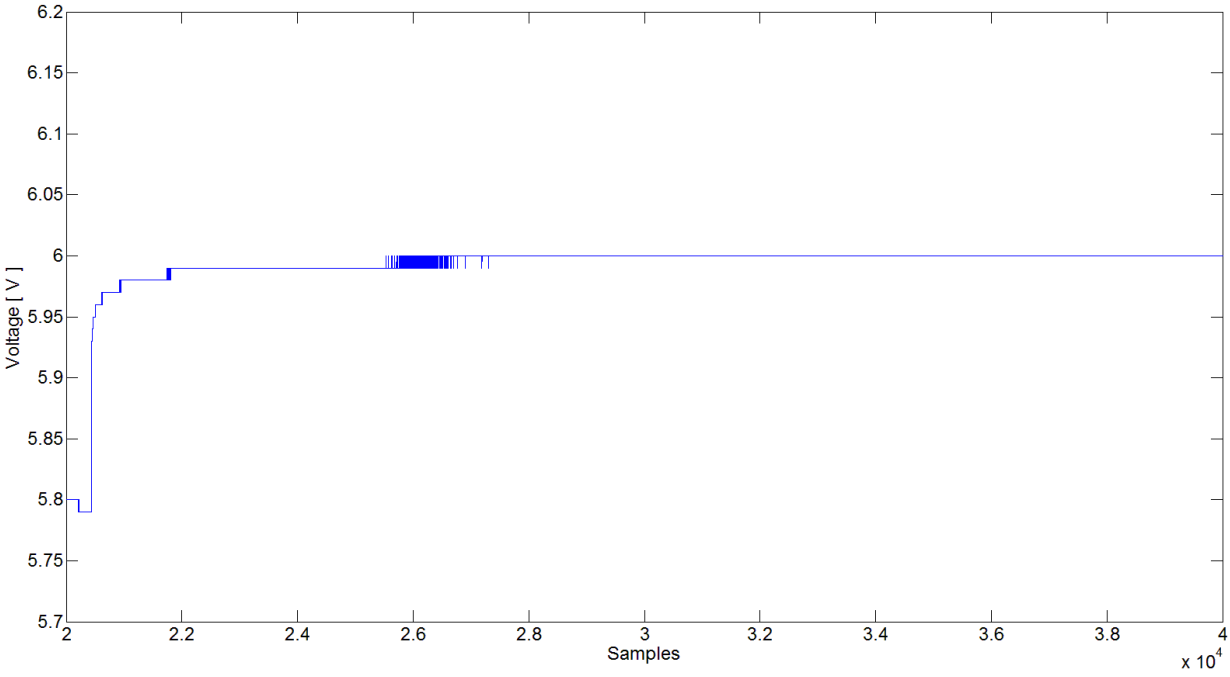

Fig. 2.5.2. The stabilization of the OCV after being disconnected from the load.

2.5.2. Specific Gravity (SG) method

Measurement of the specific gravity of the electrolyte is equivalent to testing the concentration of acid (sulphuric acid) in the electrolyte. During the battery discharging process the active material is consumed and its concentration decreases. The Specific gravity (SG) test can be performed using a traditional hydrometer, which is time consuming process and cannot be performed in a real time so another method is preferable, i.e. using a modern digital sensor, placed inside the cell, which updates the state of electrolyte continuously [16]. This method, however is only briefly described in the literature and the specific gravity/ electrolyte density proportions may vary depending on the producer of the battery [16, 19].

2.5.3. Coulomb counting method

Current integration method (also called a direct method) is a simple process of summing of capacity taken out from the battery. The current SOC of a battery is simply a maximum charge minus the current, multiplied with time for which it was flowing.

Theoretically, this method is an obvious and simple choice to implement, however, practically it has many disadvantages. The current flow is not constant, but changes with the battery operations, the longer the method is used the bigger the error gets due to the presence of an integral. Furthermore this method relies on a discharging process, thus without the knowledge of a discharge data (i.e. time, discharge current) the user is simply unable to estimate the current SOC.

2.5.4. Impedance measurement method

Impedance is another variable that characterizes a battery, which changes with charging/discharging processes. The change in active chemicals in the cell affects the change of its impedance. The measurement of a battery internal impedance is also a way to estimate the SOC, however, it is not a common strategy due to its complexity and temperature dependence [16].

2.6. Battery modeling techniques

In order to fully understand the operation of a battery different approaches must be taken, as the problems cover many fields of science. In order to help solve these problems several model types were created, amongst which the most common are:

- Electrochemical models
- Physical models
- Equivalent circuit models

Each of the presented models gives different perspective into explanation of the behavior of the battery from their respective field of science. Such separation was created so that knowledge from just one of the areas is sufficient to understand the processes taking place inside the battery.

Electrochemical models focus mostly on the chemical reactions taking place inside the battery. This type of battery model finds its use in construction and design of the battery. However, many parameters of the battery are very hard to describe using these models, such as internal resistance, which makes them not feasible to represent the dynamically changing key variables describing the battery behavior. However, the dynamic properties of battery can

be obtained by analyzing the consistency of the substances taking part in the electrochemical reaction caused by connection of electrodes to external circuit.

Physical models represent the operation of the battery through mathematical and physical equations. Two main methods used for creation of those models can be distinguished, which are the finite number and the computational fluid dynamics technology. These methods allow deep understanding of the fluid and mass flow as well as heat transfer which are important for the operation of the battery. However, high computational power is required due to many complex calculations. Moreover, the process requires a lot of time which deems the model unusable for the purposes of the project presented in this paper.

Equivalent circuit models represent the electrochemical parameters and the behavior of the system through the creation of simplified, equivalent circuit consisting of electrical elements. The simplicity of these models can vary greatly depending on the required level of precision. These models are easily adjustable to specific requirements while maintaining the lowest possible level of complexity. Equivalent circuit model was chosen for the project, due to its ability to follow the dynamically changing variables with reasonable computational power requirements. Example model of this model type, as well as its explanation was presented in the chapter 2.1.2, “Electric model of the battery”.

2.7. Electric equivalent circuit models

2.7.1. Simple battery model

A simple battery model consists of only linear, passive elements, created through the use of open-circuit voltage ideal battery and constant internal resistance, the model is shown in the figure 2.7.1.

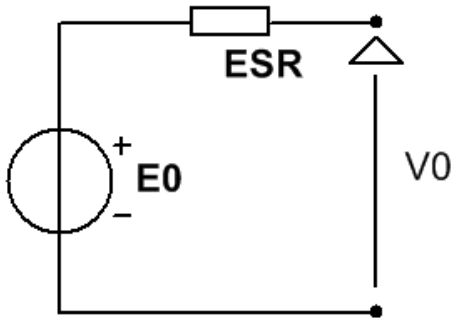

Fig. 2.7.1 Simple battery model [4]

Where :

ESR – internal series resistance

Vo – terminal voltage of the battery

Eo – open circuit voltage

The model it is mostly used in systems where the battery doesn't have too high of an influence on the circuit. It is incapable of describing the battery behavior due to the lack of the relation of internal resistance in different states of charge (SOC).

2.7.2. Advanced simple battery model

An advanced simple battery model is an improved version of the simple battery model through the addition of the dependence of internal resistance on the SOC [4]. The configuration of this model is the same as the simple battery model, presented in figure 2.7.1. The relation between the internal resistance and the SOC is represented by equation:

$$ESR = \frac{R_0}{SOC^k}$$

Where:

R_0 - resistance of the fully charged battery

SOC – state of charge of battery

k – capacity coefficient

2.7.3. Thevenin battery model

Thevenin battery model is another commonly used model which was designed to account for transient behavior of the battery. The model is shown in the figure 2.7.2. The R_0 parameter represents the resistance between the contact plates and electrolyte while the C_0 relates to the capacitance between the parallel plates [4]. The big disadvantage of the thevenin model is the assumption of constancy of all the elements, as they all depend on the SoC and other battery characteristics.

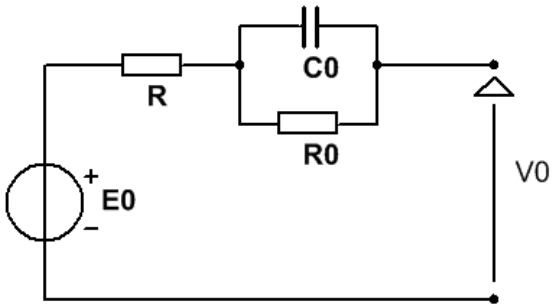

Fig. 2.7.2 Thevenin battery model [4]

Where:

E_0 – ideal battery voltage

R – internal resistance

C_0 – capacitance

R_0 – resistance between the contact plates and electrolyte

2.7.4. Modified Thevenin Model

The improvement to the basic Thevenin Battery Model has been done by Farell [2]. The improved model is presented in the figure 2.7.3.

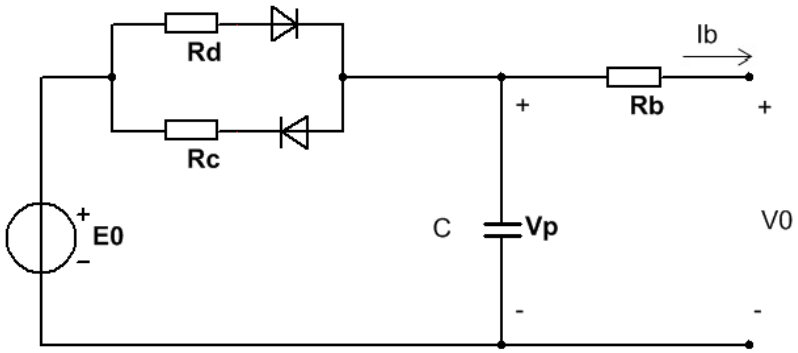

Fig. 2.7.3 Modified Thevenin equivalent circuit model [7].

The charging/discharging equations are given by

$$\frac{dV_p}{dt} = -V_p \frac{1}{R_d C} + V_0 \frac{1}{R_d C} - I_b \frac{1}{C}, \quad V_p \le V_0$$

$$\frac{dV_p}{dt} = -V_p \frac{1}{R_c C} + V_0 \frac{1}{R_c C} - I_b \frac{1}{C}. \quad V_p > V_0$$

Where:

$$I_b = \frac{V_p - V_0}{R_b}$$

R_d and R_c are two kinds of internal resistances of a battery. The diodes are used to imply that during the charging and discharging processes only one of the internal resistors will be taken into account, depending on the current flow's direction. The polarization capacitance is represented by the capacitor C. The improvements to the model enable it to account for dynamic changes taking place inside of the battery.

2.7.5. Third-Order Battery Model

A Third-Order Battery Model is presented in the figure 2.7.4.

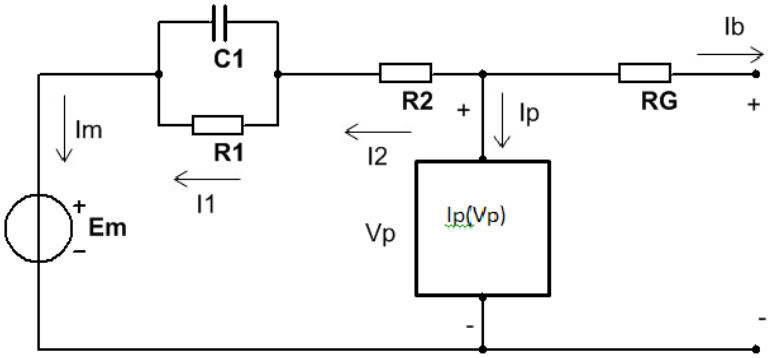

Fig. 2.7.4 A Third-Order Battery Model [7]

The model is divided into the main, and the parasitic branch. It consists of two R-C blocks, ideal source of energy (E_m) and two resistors R_2 and R_g. This model is particularly interesting due to its relation to the SOC calculation and the internal electrolyte temperature. Some of its computational elements are the functions of state of charge and the temperature, which is an unquestionable advantage comparing to the previously described models. The variables are the currents I_1 and I_2, the state of charge $Q_e$and the electrolyte temperature [7]
The dynamic equations for this model are as following:

$$\frac{dI_1}{dt} = \frac{1}{\tau_1}(I_m - I_1),$$

$$\frac{dQ_e}{dt} = -I_m$$

$$\frac{d\theta}{dt} = \frac{1}{C_\theta}\left[P_s - \frac{\theta - \theta_a}{R_\theta}\right]$$

Where :

$\tau_1 = R_1 C_1$

$C(I, \theta) = I_{avg} = I_1$

$E_m = E_{m0} - K_E(273 + \theta)(1 - SOC)$

$I_p = v_p G_{p0} e^{\left(\frac{V_p}{V_{p0}} + A_p\left(1 - \frac{\theta}{\theta_f}\right)\right)}$

And:

E_{m0}, G_{p0},V_{p0},A_p are constants for a particular battery

R_θ = thermal resistance between the battery and its environment

θ_a = temperature of the environment

2.7.6. Simplified equivalent circuit model

A simple battery model structure was introduced in [10] and is introduced in the figure 2.7.5. An author of the paper approached the problem with the simplicity-oriented attitude.

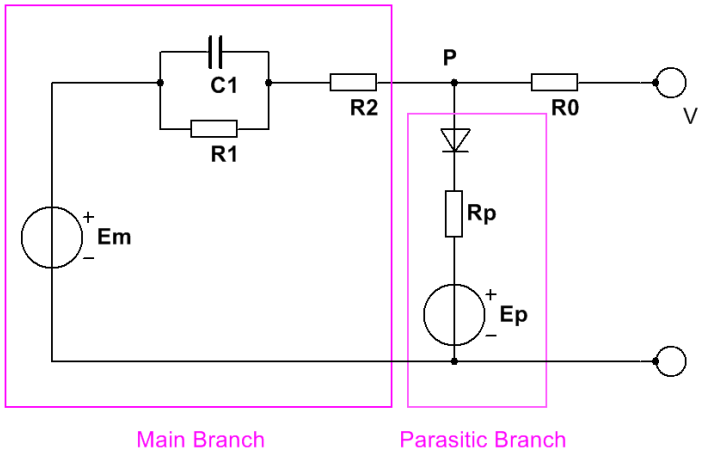

Fig. 2.7.5 The equivalent circuit model for a simplified method.

Where the relations between the variables are as following:

$E_m = E_{m0} - K_E(273 + \theta)(1 - SOC)$

$R_0 = R_{00}[1 + A_0(1 - SOC)]$

$R_1 = -R_{10} \ln(DOC)$

$C_1 = \frac{\tau_1}{R_1}$

$R_2 = R_{20} \frac{\exp[A_{21}(1 - SOC)}{1 + \exp\left(A_{22} \frac{I_m}{I^*}\right)}$

$$I_p = V_{PN} G_{p0} exp\left(\frac{\frac{V_{PN}}{\tau_p s+1}}{V_{p0}} + A_p + \left(1 - \frac{\theta}{\theta_f}\right)\right)$$

And :

E_{m0} = open circuit voltage at full charge
K_E = constant
θ = electrolyte temperature
R_{00} = value of R_0 at SOC = 1
τ_1 = main branch time parameter in seconds
I_m = main branch current
I* = nominal battery current
A_0,K_E, R_{10}, R_{20}, A_{21},A_{22}= constant

Introduced structure does not take the lead-acid battery's internal chemical processes into account, however, it temporarily approximates the processes which may be observed during the battery work. It consists of two circuits: the main branch approximating the battery dynamics in typical circumstances, and a parasitic branch, which imitates the battery behavior at the end of its charging. Every element of the circuit is based on non-linear mathematical representation and is a function of SOC, DOC (depth of charge) or temperature. The equations' variables are dependent on the determined constants. The electrolyte temperature, voltages, currents and stored charge are regarded to as states.

3. Algorithm design and implementation

In the beginning of this chapter the problem will be presented and analyzed. In the next step, the requirements for the algorithm will be introduced, leading to a theoretical design of a suitable and implementable algorithm, which fulfills the specifications. In order to have a comparison, an alternative method will be chosen, presented and described in details. It will later be used in the testing phase to provide alternative SOC estimation tool and a method to be compared with. The final part of the chapter will include the detailed description of a laboratory setup, which was used for both implementation and testing. As a chapter's conclusion, the practical, step by step instruction covering the implementation of a designed SOC estimation algorithm will be introduced.

3.1. Project requirements

To enlist the requirements the problem must be first described and analyzed. With the cooperation of a Swedish company - Micropower (www.micropower.se) - Research and Development department the problem of an electric forklift's Lead-Acid Batteries SOC and SOH will be introduced.

First of all, Electric Vehicle acts as a highly variable load so the current drawn from a battery is not constant during the discharge phase. The designed SOC and SOH estimation software should operate in real-time, providing the forklift's operator with the crucial information - the SOC and SOH of the battery at any given moment.

The method will be designed and tested in Mathworks MatLab® environment, the project group will try to ensure that it is translatable and implementable in C programming language. Such solution would make it possible to be added as a feature for the operator's onboard Human - Machine Interface.

Typical voltage and current curves during the battery discharge are presented in the figure 3.1.1. Presented data was gathered during the real forklift's operations in Micropower. The sampling interval is 4 minutes, which is too long for a data to be called precise and thus useful in the tests as not accounting for changes during those periods may increase the error in SOC estimation. However, it clearly shows the changes in load during the discharge phase of a forklift's battery.

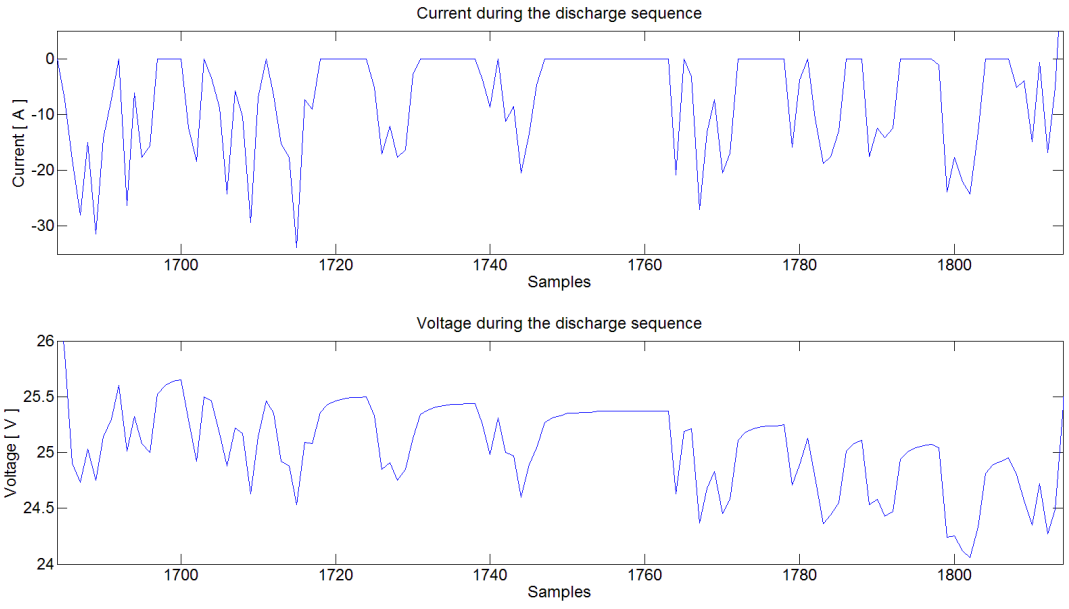

Fig. 3.1.1 Voltage and current discharge curves during forklift's operation with 24V battery.

There is no apparent pattern in current drawn during the battery discharge, it depends on the load that the forklift provides during its operation. The current values vary between 0A and 32A throughout the pictured 142 samples (9 hours of operations, regular work day). There are moments in which the battery is put on hold, when the current drawn is lowered to 0A and the voltage slowly stabilizes to finally become the Open Circuit Voltage. In those moments the OCV/SOC linear characteristic can be used to provide a reliable SOC estimation.

Terminal Voltage (a measured voltage, when a battery is under load for a certain time, also called closed circuit voltage (CCV)) is highly dependent on a load. Furthermore, TV/SOC characteristic is nonlinear and depends on the battery type, nominal capacity, temperature and load, making it less useful than the OCV/SOC characteristic. For this dynamical part of voltage characteristic the Coulomb Counting method or its improved variations can be successfully applied.

The fully charged 24V battery’s Terminal Voltage is around 24,8V and the cut-off TV is around 24,1V, which is approximated to 20% SOC point. This specific value is optimal to stop discharging the battery in order to ensure that deep discharge does not occur. Avoiding the deep discharge is highly desired by the customer as it greatly prolongs the battery’s life.

Micropower's Battery Monitoring Unit (BMU) will be used as a measurement tool in the project. It provides the user with the real-time voltage, current and internal temperature measurements and transfers the data via Wi-Fi, communicating with the company's software installed on the PC.

Although the project focuses on the discharging process (estimating the battery SOC while it is under discharge) data gathered during the charging process may also be of use. The main charging peak consists of around 45 first samples, the rest of the process are the "maintenance" current spikes. During 3 hours the battery is loaded with certain pattern. The usefulness of the charging curve lies within the information on how much Ampere-hours have been transferred to the battery and what value the OCV have after the charging is finished. Those two information will be used in the algorithm to improve its performance. Several equivalent circuit models use the current measurement to estimate the battery internal temperature and voltage. There is no need to estimate values, which can be successfully measured with the BMU so the focus in this project will be put on using all the available measurements to estimate SOC and SOH. The charging phase of the very same battery is presented in the figure 3.1.2.

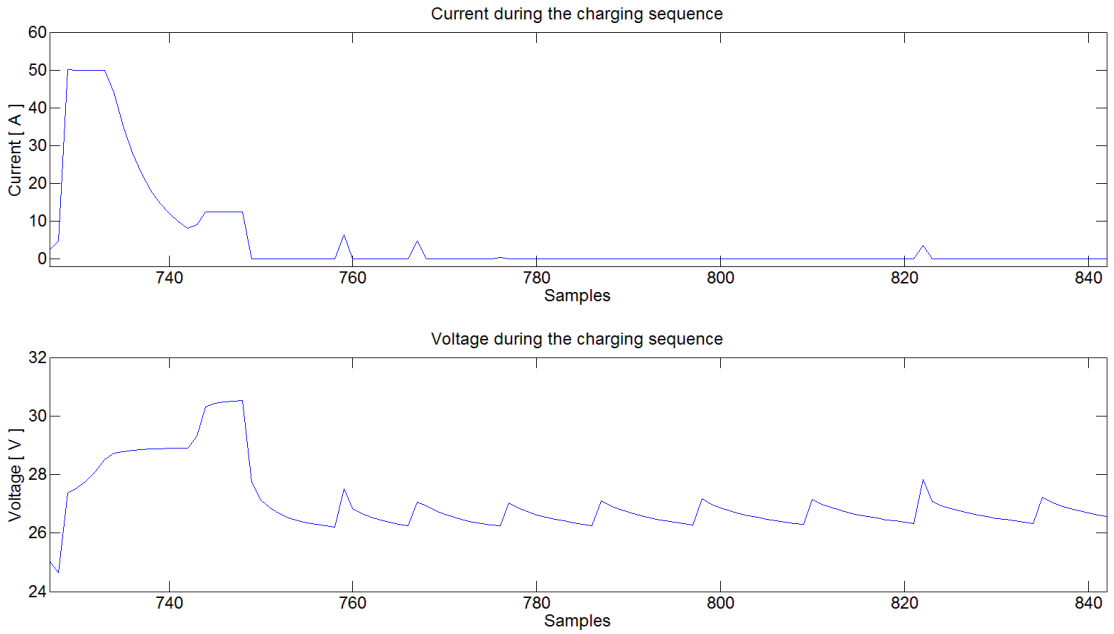

Fig. 3.1.2 Voltage and current charging curves during forklift's operation with 24V battery.

To conclude the requirements for the project will be enlisted below:

- The Method's precision of minimally 5% is allowed. 5% error in SOC estimation ensures that the battery will never be discharged far below 20% of its SOC, which is critical in order to keep the battery performance at a certain point and avoid the deep discharges,
- No parameterization should be required in order to start using the algorithm. It is crucial for the company not to be forced to conduct any parameterization process for each kind of batteries the customer may use. Parameterization will only be done for a comparison of an equivalent circuit method and used once in the testing phase to compare the two methods precision and reliability,
- All the available measured variables should be used (Voltage, current drawn and the internal temperature)
- The algorithm should not require any specific input from the operator. The initial capacity and battery nominal voltage should be measured and estimated by the algorithm itself during the first cycles of operation,
- The final form of the designed algorithm should be as simplified as possible. Even though complex algorithms (such as Fuzzy Reasoning and Extended Kalman Filter) may be of use in the project the final form should be simplified and implementable in C programming language,

- All the measurements will be done by the Micropower BMU and then transferred and processed in MatLab environment in order to conduct the tests.

3.2. Reference method

It was decided that the designed method will be compared with another one from the literature. The OCV estimation method, based on the article "Estimating the State of Charge of a Battery" by John Chiasson and Baskar Vairamohan, published in "Transactions on Control Systems Technology" was chosen as a reference. A Modified Thevenin circuit was used for modeling the battery's behavior as it accounts for energy losses in all forms as well as the transient behavior of the internal current of the battery. In this section a more in-depth theoretical description of the model will be given as well as the algorithm for the method. Practical implementation of the model in MatLab environment will be presented in the section 2.5 "Implementation".

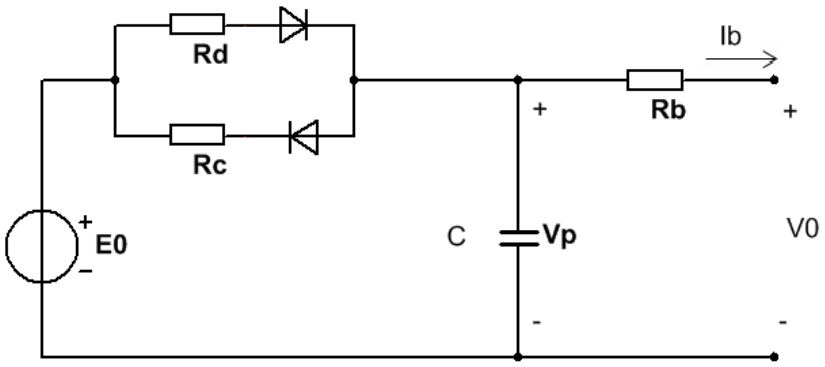

Fig. 3.2.1 Modified Thevenin equivalent circuit model [7].

The description of basic electric elements present in the model was given in section 2.7.4, electric equivalent circuit is presented in figure. 3.2.1. However, it should also be noted that the polarization capacitance C is not purely electrical capacitance as portion of it is due to chemical diffusion within the battery. Energy loss in the battery in all forms is modeled through the use of three resistances: R_c, R_d, R_b which stand for charge, discharge and terminal resistance respectively. The terminal current of the battery I_b have positive values during discharge process [5].

The purpose of the method is to estimate the battery's SOC based on OCV assuming that only terminal voltage and current can be directly measured. It also should be stated that parameters: R_c, R_d, R_b, C, V_p are neither known a priori nor can be measured. The algorithm of the method will be presented in several steps. In this paper, a short summary of the method will be presented. It is strongly based on [5] and more detailed information can be found there.

1). Define the state variables:

$$x_1 = V_p, x_2 = \frac{1}{R_d C}, x_3 = \frac{V_{OC}}{R_d C}, x_4 = \frac{1}{C}, x_5 = R_b \quad (1)$$

Where:

V_p – capacitance voltage
R_d – discharge resistance
R_c – charge resistance
R_b – terminal resistance
C – polarization capacitance

2). Create nonlinear time-varying state-space model:

$$\dot{x}_1 = -x_1 x_2 + x_3 - I_b(t) x_4$$

$$\dot{x}_2 = 0$$

$$\dot{x}_3 = 0$$

$$\dot{x}_4 = 0$$

$$\dot{x}_5 = 0$$

$$V_b = x_1 - I_b(t) x_5$$

Where :

$x(0) = (x_{10}\, x_{20}\, x_{30}\, x_{40}\, x_{50})^T$ is unknown,

The open circuit voltage can be derived from (1).

3). Create the system in the form of:

$$\frac{d}{dt}\begin{bmatrix} z_1(t)) \\ z_2(t)) \\ z_3(t)) \\ z_4(t)) \end{bmatrix} = \begin{bmatrix} -x_{20} & 1 & -I_b(t) & 0 \\ 0 & 0 & 0 & 0 \\ 0 & 0 & 0 & 0 \\ 0 & 0 & 0 & 0 \end{bmatrix} \begin{bmatrix} z_1(t)) \\ z_2(t)) \\ z_3(t)) \\ z_4(t)) \end{bmatrix}$$

$$z(t_0) = \begin{bmatrix} x_{10} \\ x_{20} \\ x_{30} \\ x_{40} \end{bmatrix} y(t) = \begin{bmatrix} 1 & 0 & 0 & -I_b(t) \end{bmatrix} \begin{bmatrix} z_1(t) \\ z_2(t) \\ z_3(t) \\ z_4(t) \end{bmatrix}$$

Where : $z_1 = x_1$, $z_2 = x_3$, $z_3 = x_4$, $z_4 = x_5$.

The reason for excluding the state x_2 is presented in the step 6. The exact value of the state is presented in equation (1).

4). Definition in order to Check the observability of the system

Firstly, the system is to be rewritten in a more compact form:

$$\frac{dz}{dt} = A(t) * z(t) \quad (2)$$
$$z(t_0) = (x_{10,}x_{30,}x_{40,}x_{50}) \quad (3)$$
$$y(t) = C(t) * z(t) \quad (4)$$

Where:

$$A(t) = \begin{bmatrix} x_{20} & 1 & -I_b(t) & 0 \\ 0 & 0 & 0 & 0 \\ 0 & 0 & 0 & 0 \\ 0 & 0 & 0 & 0 \end{bmatrix} \qquad C(t) = \begin{bmatrix} 1 & 0 & 0 & -I_b(t) \end{bmatrix}$$

Secondly, transition matrix of the system is defined as:

$$z(t) = \Phi(t) * z(t_0) \quad (5)$$
$$y(t) = C(t) * \Phi(t) * z(t_0) \quad (6)$$

Where:

$$\frac{d\Phi(t)}{dt} = A(t) * I|(t) \quad (7)$$

$$\Phi(t) = I_{n\times n} \tag{8}$$

The system is observable on $[t_0,t_f]$ if and only if the Gramian matrix M is invertible [5].

$$M(t) \triangleq \int_{t_0}^{t_f} \Phi^T(t) * C^T(t) * \Phi(t)dt \tag{9}$$

If the matrix M is invertible, the initial values of $z(t_0)$ can be found through the integration of a multiplication of y(t) by $I|^T(t) * C^T(t)$:

$$M(t) * z(t_0) = \int_{t_0}^{t_f} \Phi^T(t) * C^T(t) * y(t)\, dt \tag{10}$$

$$z(t_0) = M(t)^{-1} \int_{t_0}^{t_f} \Phi^T(t) * C^T(t) * y(t)\, dt \tag{11}$$

5). Find conditions for non-singularity of the Gramian

In order to calculate the $z(t_0)$ the matrix M must be non-singular, the process of finding the conditions for such feature is as follows:

By solving the equation (7) for $\Phi(t)$:

$$\frac{d\Phi_{11}}{dt} = -\Phi_{11}x_{20} \tag{12}$$
$$\frac{d\Phi_{12}}{dt} = -\Phi_{12}x_{20} + 1 \tag{13}$$
$$\frac{d\Phi_{13}}{dt} = -\Phi_{13}x_{20} - I_b(t) \tag{14}$$
$$\Phi_{14} \equiv 0 \tag{15}$$

With:

$$\Phi_{ij} = \delta_{ij}, \quad \text{i = 2,3,4 and j = 1,2,3,4} \tag{16}$$

Results in :

$$\phi(t) = \begin{bmatrix} \phi_{11} & \phi_{12} & \phi_{13} & 0 \\ 0 & 1 & 0 & 0 \\ 0 & 0 & 1 & 0 \\ 0 & 0 & 0 & 1 \end{bmatrix}$$

Where:

$$\Phi_{11} = e^{-x_{20}(t-t_0)}\,,\ \Phi_{12} = \frac{1}{x_{20}} * (1 - e^{-x_{20}(t-t_0)}),\ \Phi_{13} = -\int_{t_0}^{t} e^{-x_{20}(t-\tau)} * I_b(\tau)d\tau$$

Assume that over any short time interval, the battery current waveform can be fit to quadratic equation:

$$I_b(t) = a + b(t - t_0) + c(t - t_0)^2 \tag{17}$$

If we combine (17) with the definition of $I|_{13}$ we get:

$$\Phi_{13}(t) = \frac{2c - bc^2 + ax^2{}_{20}}{x_{20}{}^3} * e^{-x_{20}(t-t_0)} - \frac{1}{x_{20}{}^3}(2c - bx_{20} + ax_{20}{}^2 - 2cx_{20}(t - t_0) + bx_{20}{}^2(t - t_0) + cx_{20}{}^2(t - t_0)^2)$$

$$M(t) = \int_{t_0}^{t_f} \begin{bmatrix} \phi_{11}^2 & \phi_{11}\phi_{12} & \phi_{11}\phi_{13} & -\phi_{11}I_b(t) \\ \phi_{12}\phi_{11} & \phi_{12}^2 & \phi_{12}\phi_{13} & -\phi_{12}I_b(t) \\ \phi_{13}\phi_{11} & \phi_{13}\phi_{12} & \phi_{13}^2 & -\phi_{13}I_b(t) \\ -I_b(t)\phi_{11} & -I_b(t)\phi_{12} & -I_b(t)\phi_{13} & I_b(t) \end{bmatrix}$$

6). Calculation of the OCV

As $V_{OC} = \frac{x_{30}}{x_{20}}$, however it was proven in [5] that the V_{OC} is not asymptotically dependent of x_{20}. The given solution to the problem was to use arbitrary value of $\overline{x_{20}}$ in equation (17)

$$V_{OC} = \lim_{t_f - t_0 \to \infty} \left(\frac{1}{x_{20}} * [0\ 1\ 0\ 0] M^{-1}(t) * \int_{t_0}^{t_f} \Phi^T(t) * C^T(t) * y(t) dt\right) \tag{18}$$

3.3. Designed method

For the time being, the Battery Monitoring Unit (BMU) uses well-established coulomb counting method in order to calculate the remaining State of Charge of the battery during discharge. As the currently implemented algorithm produces error, which is unacceptable in forklift's operations, it is reasonable to improve it. The designed algorithm is based on the very same coulomb counting, but also the measurements, which are currently unused, such as terminal voltage and the battery internal temperature.

The algorithm was designed during laboratory discharge tests and bases mostly on observations and empirical knowledge. In [9] the authors used similar approach, creating a method that corrects the SOC readings depending on the discharge current profiles. The method presented in the paper is called "Enhanced Coulomb Counting" and works well with

the discharges under constant load. As mentioned before, the forklift's operations include the nonlinearly-changing load, making the method from [9] not valid for our application.

Although the coulomb counting method is widely used, it generates relatively high error and is too dependent on the ampere-meter readings, and thus is not reliable as a stand-alone method. On the other hand, there is an almost linear OCV/SOC relation, which gives solid results with very low error values. However, in order to obtain open circuit voltage readings, the battery must be disconnected from the load for a certain amount of time, what hardly ever happens in forklifts daily operations. The algorithm can be regarded to as "Improved Coulomb Counting" as it uses the coulomb counting as a primary method, but corrects it with the correction factor. Its values depend on the error between the SOC calculated with Ah counting and SOC derived from OCV/SOC diagram.

Typical forklift's daily operations consist of around 9 hours under variable load with numerous breaks, each being too short to estimate the battery's OCV with a sufficient precision. Those breaks enable the algorithm to estimate the OCV from the "Semi-OCV" values that occur after a certain amount of time without flow of the current. Typical battery voltage behavior after disconnection from the load is presented in the figure 3.3.1.

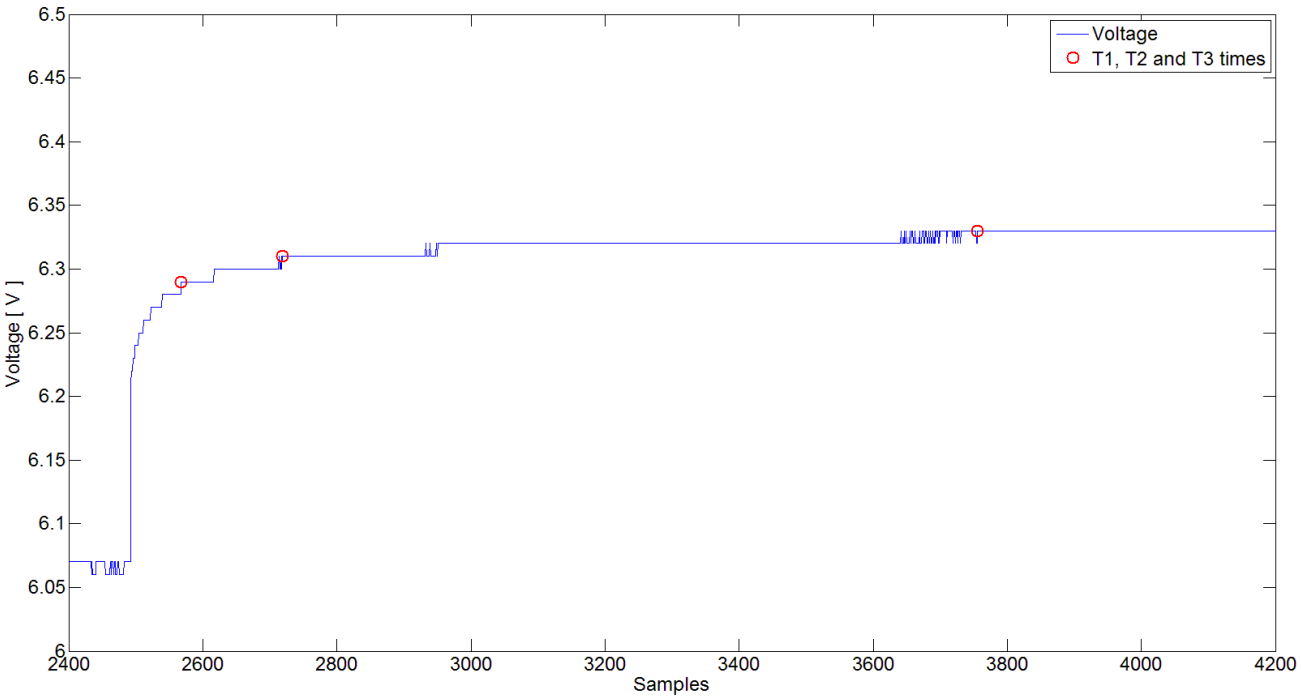

Fig. 3.3.1 Battery Voltage after being disconnected from load.

The sample time is set to 2s. The graph presented in figure 3.3.1 covers around 1800 samples, which is 1 hour of data collection. The red dotted points, namely T0, T1, T2, T3 are pre-counted points referring to:

- T0 - first sample when the current has 0 value,
- T1 - the moment, when the voltage starts being constant for 30 samples (60 seconds),
- T2 - the moment, when the voltage starts being constant for 150 samples (5 minutes),
- T3 - the moment when the voltage starts being constant for 2700 samples (90 minutes).

Those 4 points must be pre-counted, i.e. the algorithm needs a long (preferably more than 2 hours) rest after the first discharge. It has been proven that the real Open Circuit Voltage value might be measured after 1.5 hours with the battery disconnected from the load, and the changes dynamics had not changed over numerous discharge tests (Figures 3.3.1 - 3.3.6). T1, T2 and T3 had been counted from T0. Those numbers are intervals between the moment battery is put on "hold" and the voltage is constant for a certain amount of time.

As pictured in the figure 3.3.1, the voltage does not change significantly between the T1, T2 and T3 points. The voltage in T3 moment is 0.02V higher than in T2 point and 0.04V higher than in T1 point. This relationship has been proven correct, no matter what the discharging current values were before the battery was put on hold and how long the discharge lasted. This similarity is used in the algorithm, ex. even if the rest time of the battery is much shorter than required in order to measure the OCV, its value can be estimated after reaching the T1 point (which in this case was 74 samples, around 2.5 minutes). The relation between the voltages in T3, T2 and T1 points for the different discharge curves is shown in the table 3.3.1.

#	Figure	Diff1 (T3-T1) (V)	Diff2 (T3-T2) (V)	OCV (V)	Discharge (Ah)	Discharge Current (A)	Discharge time (s)
1	3.3.2	0.03	0.01	6.16	2.43	5	1753
2	3.3.3	0.04	0.02	6.00	81.18	11	26589
3	3.3.4	0.04	0.02	6.00	118.56	13	32840
4	3.3.5	0.04	0.02	6.03	13.68	14	3520
5	3.3.6	0.03	0.02	6.19	27.9	14	7178

Tab. 3.3.1. Comparison between the Diff1 and Diff2 throughout various discharge periods.

Although the general trend is followed the Diff1 and Diff2 voltages may differ significantly between the tests – as Diff2 between #1 and #2 – 0.01 in value, but 100%

difference. That is why using Diff1 and Diff2 parameters will enable the algorithm to estimate, not to define the precise SOC value in any given point of time.

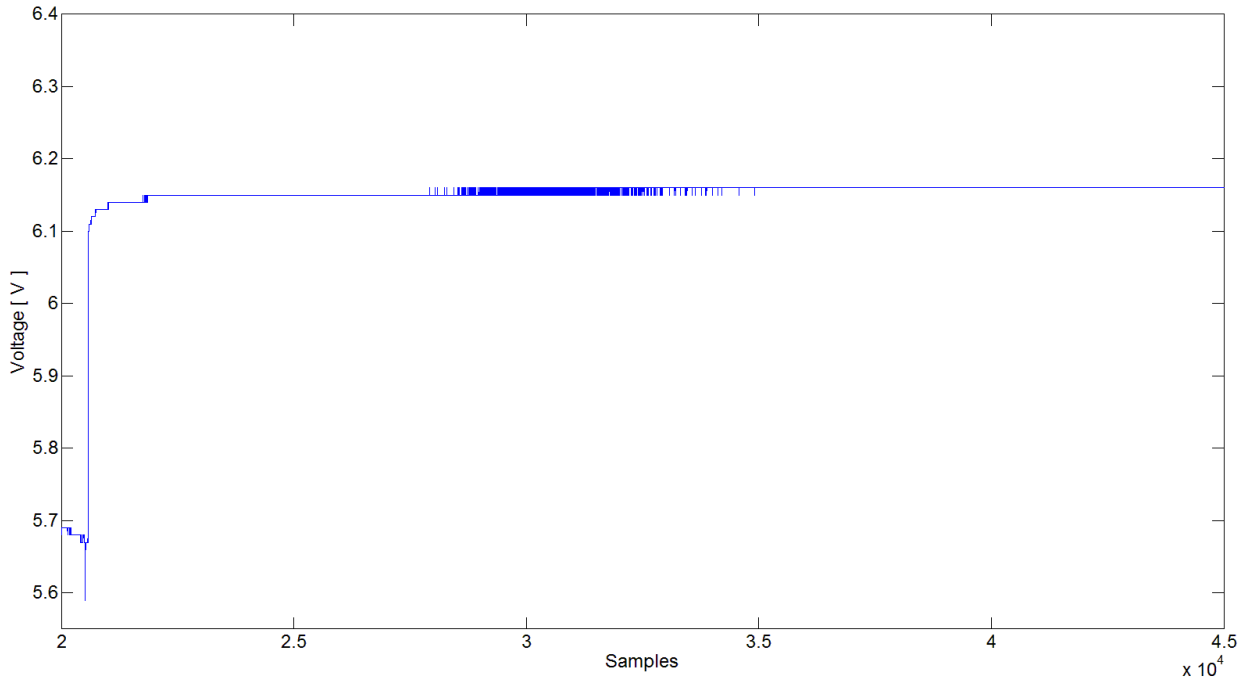

Fig 3.3.2. Voltage after disconnecting battery from the load (5A, 30 minutes discharge).

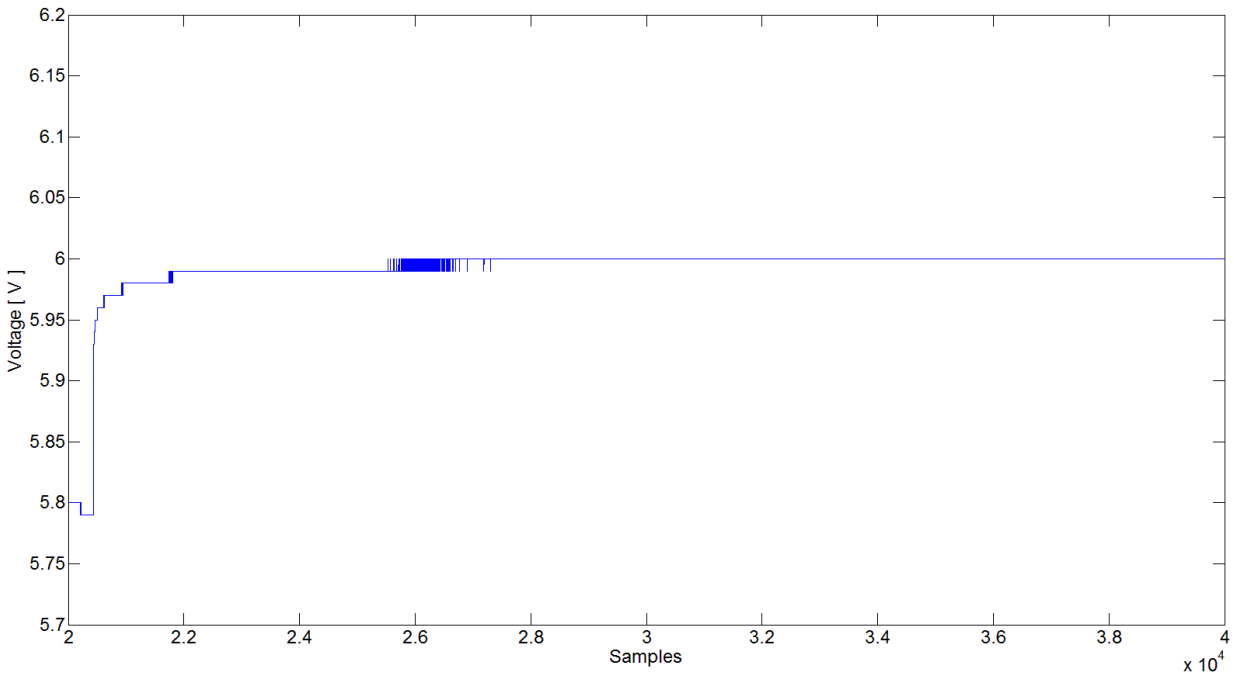

Fig 3.3.3. Voltage after disconnecting battery from the load (11A, 8 hours discharge)

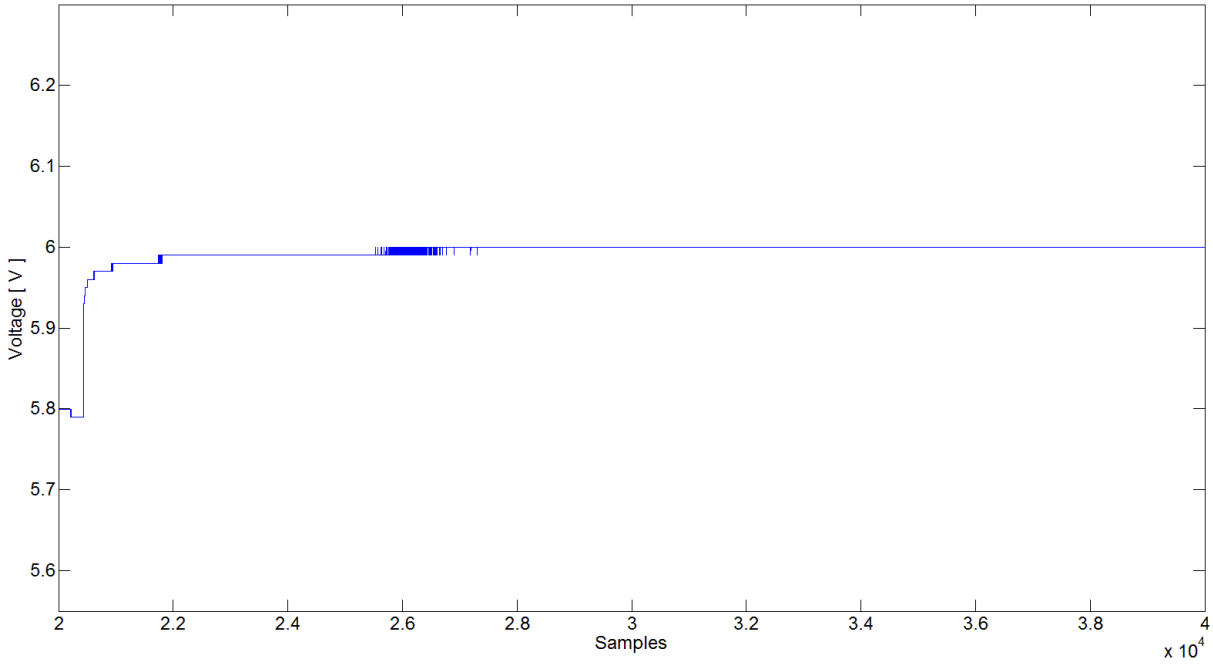

Fig 3.3.4. Voltage after disconnecting battery from the load (13A, 10 hours discharge).

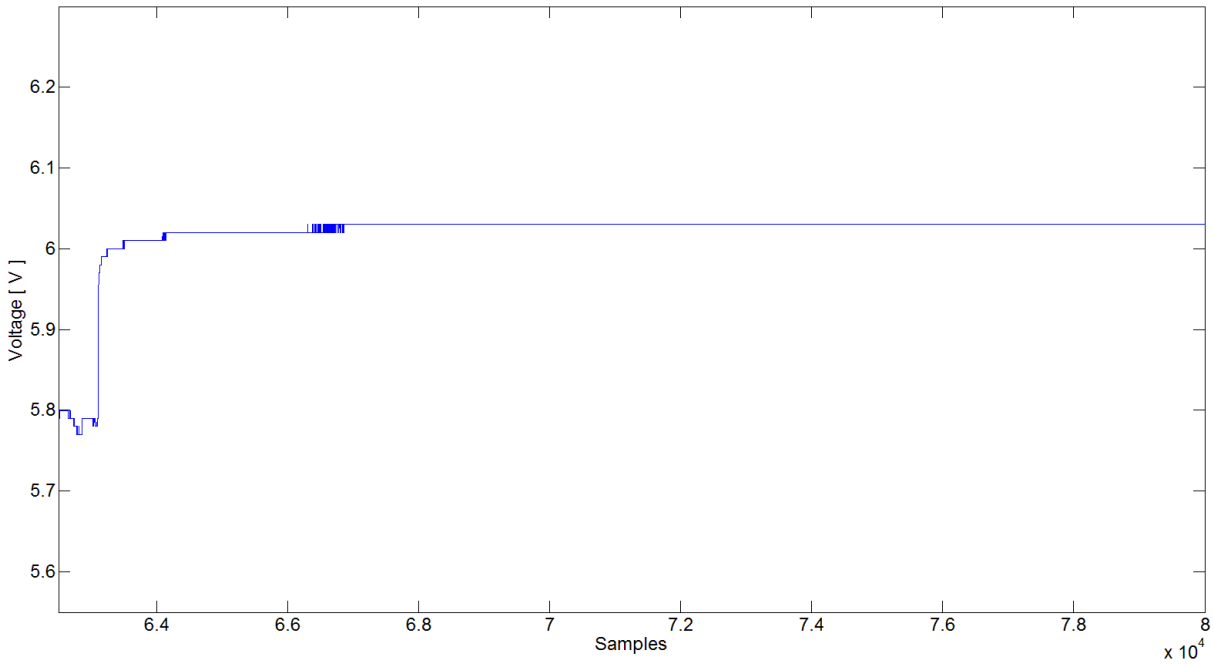

Fig 3.3.5. Voltage after disconnecting battery from the load (14A, 1 hour discharge).

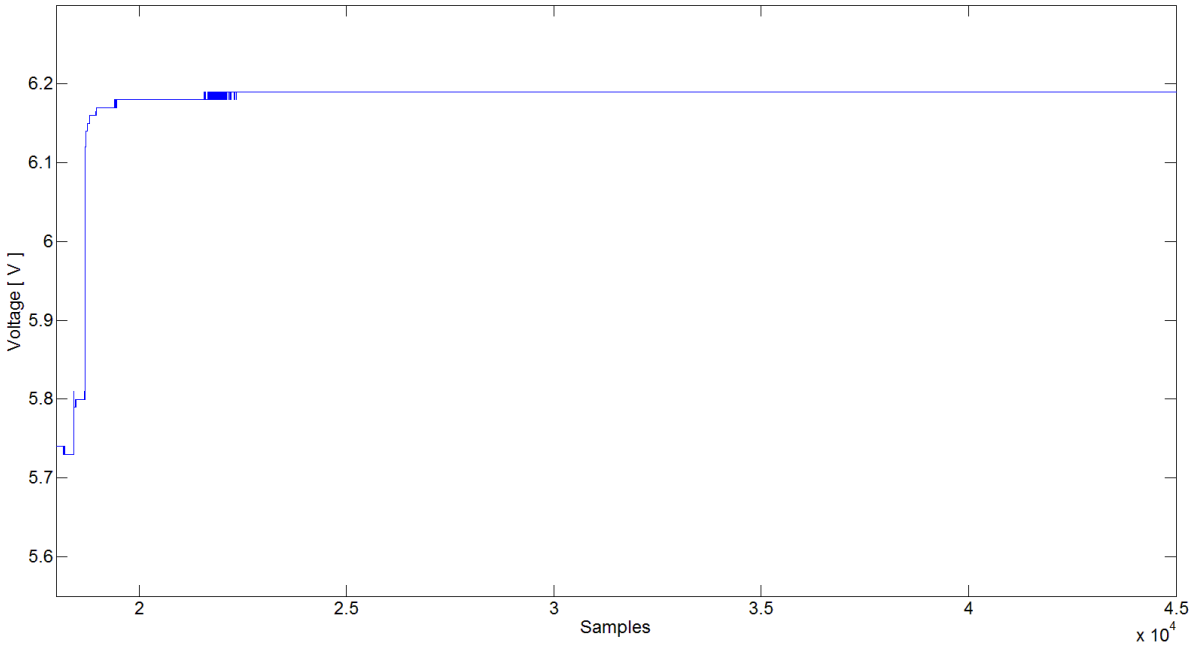

Fig 3.3.6. Voltage after disconnecting battery from the load (14A, 2 hours discharge).

The flowchart presenting the algorithm is presented in the figure 3.3.7.

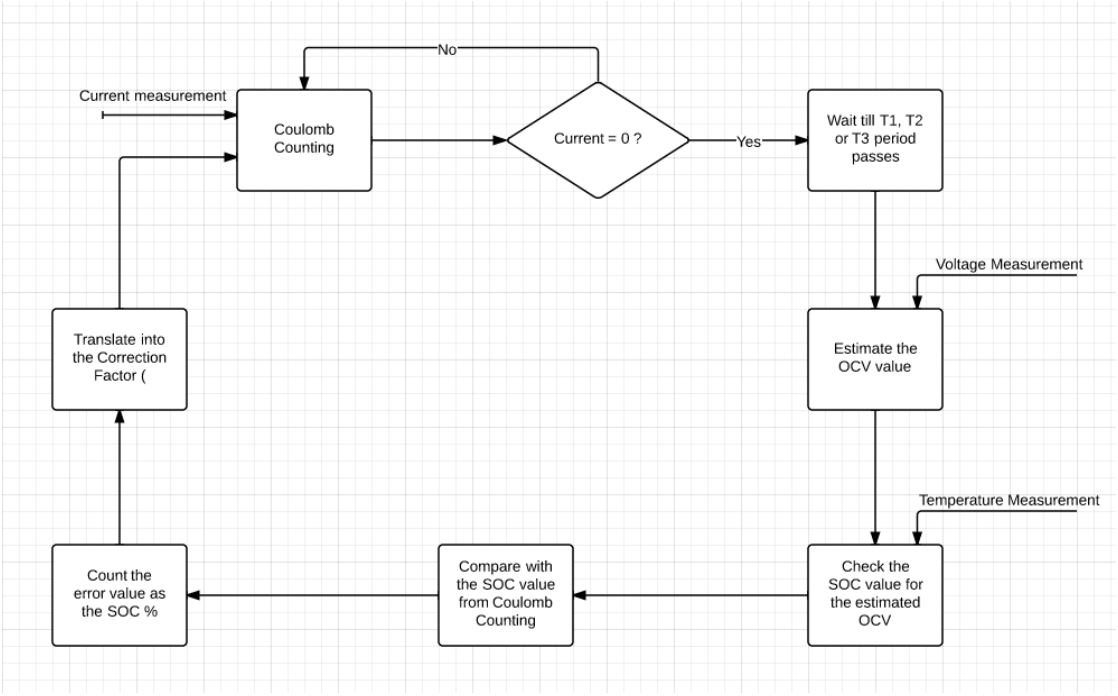

Fig. 3.3.7 Flowchart presenting the logic of the algorithm's SOC correction.

The detailed instruction for implementing the algorithm is attached below:

1. During the first measured cycle of the battery, the operator has to be cautious as the only source of SOC estimation is regular coulomb counting method. Thus it is

recommended to stop the discharge at least 10% before the SOC indicator reaches the 20% point. After the first discharge, battery should rest for at least 6 hours to enable the algorithm to calculate the T1, T2 and T3 times.

2. After the T1, T2 and T3 delay times, as well as the voltage differences at those points are saved in the memory, algorithm may proceed to the regular operation state.
3. During the regular algorithm's operations the SOC calculation is done based on the basic coulomb counting. Ampere-hours drawn from the battery are added until the moment load is disconnected. When battery is put on "hold" the correction factor has to be counted.
4. If the discharge break is short, but long enough for the T1 period, OCV is estimated based on the T1, by adding the previously counted difference (between T1 and T3 voltages) to the measured voltage. If the break continues and the T2 time passes the algorithm updates by estimating the OCV in the T2 period the same way as with T1. If the break lasts until the T3 time the measured voltage is taken as a real OCV, improving the correction's precision.
5. The difference between counted Ampere-Hours sum divided by the SOH/Nominal Voltage (giving the SOC estimate) and the previously estimated OCV translated to SOC, using the SOC/OCV linear relation forms an error. It needs to be corrected during the next hour of discharge in order for the SOC jumps to be avoided and make the change look natural for the forklift operator. The other possible solution would be to show the best known value to the operator, even though it will most form a “jump” on SOC diagram.
6. The correction factor is counted using the error value and the average current throughout the discharge:

$$Correction\ \ Factor\ =\ \frac{Avg.\ \ Current\ +\ Error^{*}}{Avg.\ \ Current}$$

*As Ah/hour

7. For the next 1 hour, the current drawn is multiplied by this factor in order to reduce the error caused during the last period of the discharge. Note that the correction is done backwards and the factor is used delicately in order to avoid the jumps in the current value and huge differences of the Ah-counting acceleration.

3.4. Laboratory setup

The main idea behind laboratory setup was to create the environment that could simulate the forklift's behavior and gather the measurements with sufficient precision. Testing stance is presented in the figure 3.4.1 and consists of:

- Switchable resistor cabinet (0.4 - 3 Ohm) as a load
- Micropower's BMU with the 12V battery power supply as a measurement unit
- 3x 4EPzS 240Ah 2V cells in series, forming the 6V 240Ah Battery
- Micropower's SMP PRO Battery Charger (Input 1x220-240V, 50-60Hz, 9A; Output 6...48V DC, 0...30A)
- PC with a Wi-Fi connection and BMU as a data collector

A zoom-in of a circuit during the discharge is presented in the figure 3.4.2 and the electrical circuit drawing in both charge and discharge status is pictured in the figure 3.4.3.

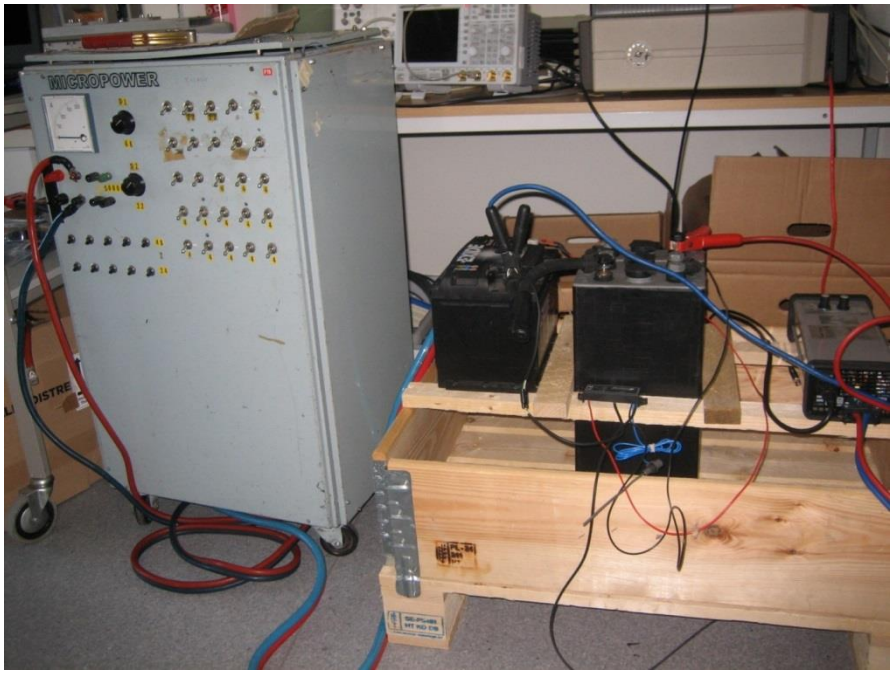

Fig. 3.4.1 Testing stance. Switchable load, 12V BMU supply battery, 6V testing cell battery, Micropower's BMU and a battery charger.

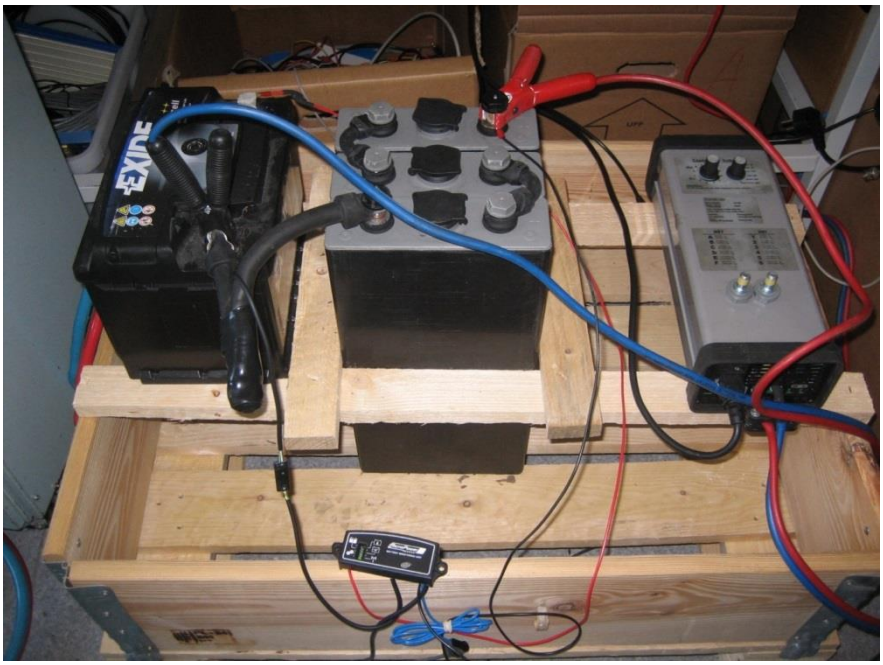

Fig. 3.4.2 Zoom-in of the testing stance during the battery charging.

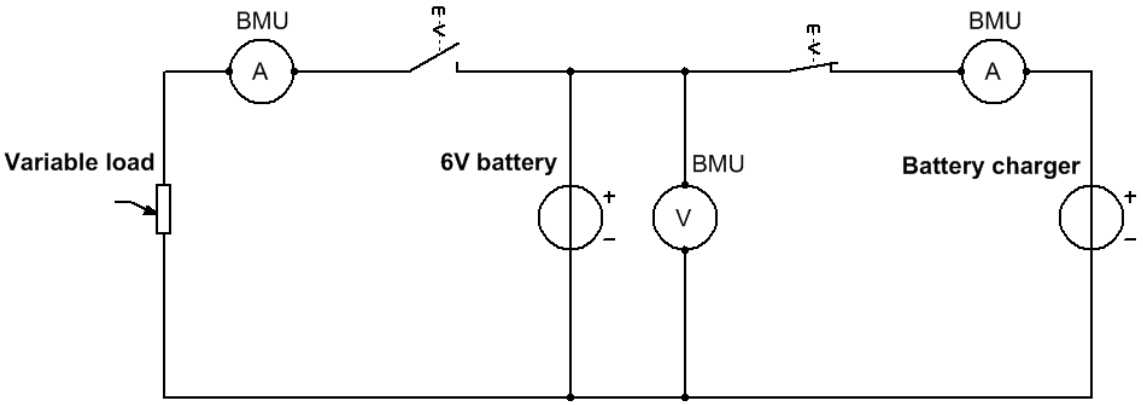

Fig. 3.4.3 Electrical circuit of a testing stance.

E-V switch position indicates the charge/discharge status of the test. Primary circuit does not include BMU's power supply. Secondary circuit is presented in the figure 3.4.4 and includes only the BMU and its 12V power supply battery.

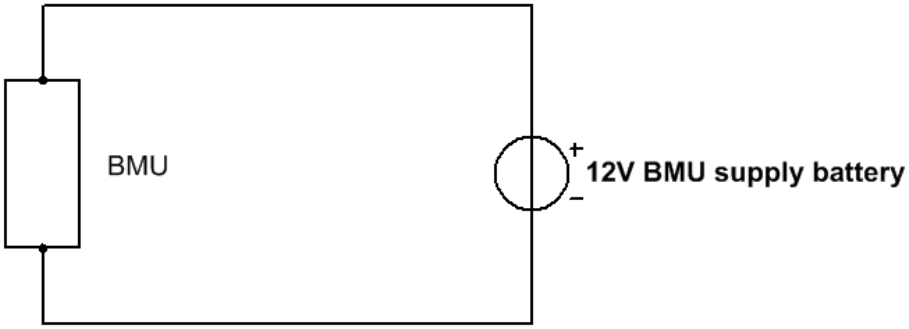

Fig. 3.4.4 BMU power supply circuit

Battery Monitoring Unit is capable of measuring both the Battery Voltage and Current. Data collection is run with a sampling time of 2 seconds, which is enough to capture even the slight changes of a current drain and the terminal voltage of the battery. The example of a collected data, plotted in MatLab is presented in the figure 3.4.5

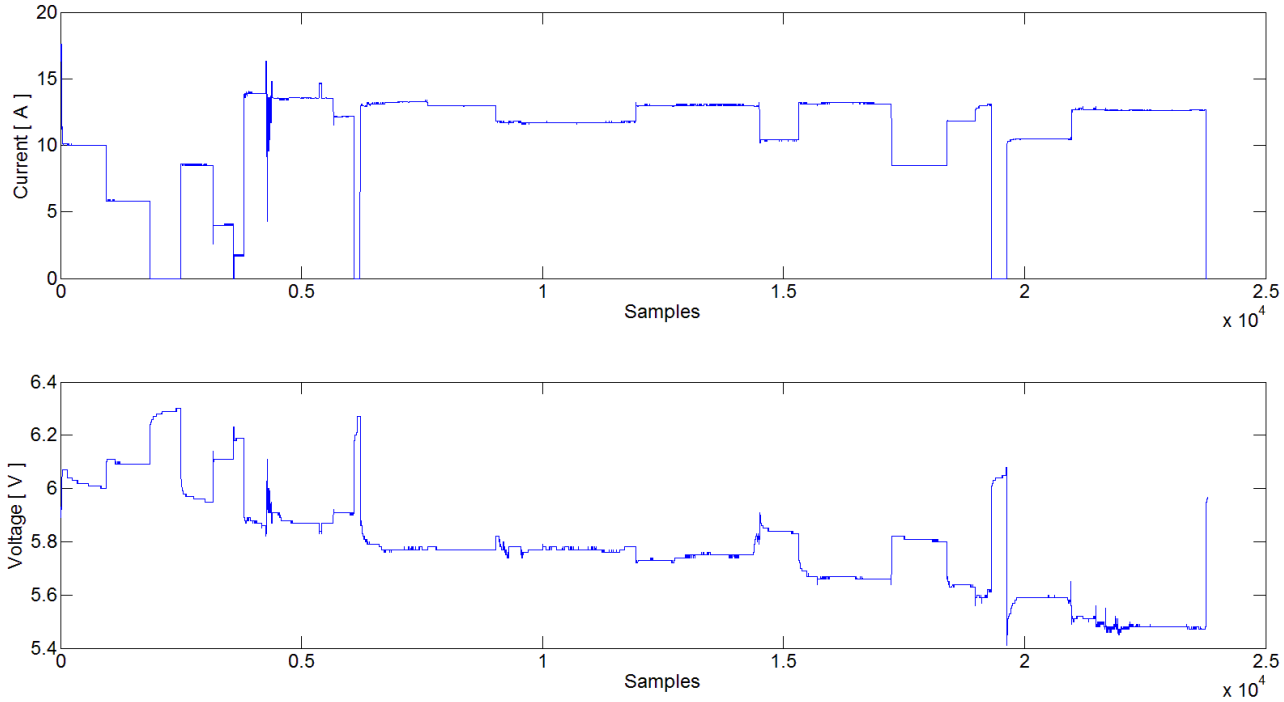

Fig. 3.4.5 Characteristic example collected with the testing stance.

3.5. Implementation

3.5.1. Reference Method MatLab Implementation

In this section, the practical implementation of the reference method will be presented. The theoretical background of the method and the equations upon which it is based were presented in section 3.3. Matlab R2012a environment was used in order to implement the method. Firstly, the program written in the m-file will be presented in the figure 3.5.1:

```
%Reading the data
clc;
clear;
f = fopen('ocvevery20.csv', 'rt');
C = textscan(f,'%s %s %f %f %s %f %s %s %f %s', 'delimiter' ,';', 'Headerlines', '1');
fclose(f);

AvgCurrent = C{1,3};
AvgVoltage = C{1,4};
a = size(AvgCurrent);
j=1;

for i=1:a(1,1)
    if mod(i,2)==1
        Current(j,1)=abs(AvgCurrent(i,1));
        end
        j=j+1;
    end
end

j=1;

for i=1:a(1,1)
    if mod(i,2)==1
        Voltage(j,1)=AvgVoltage(i,1);
        j=j+1;
    end
end

x20 = 3;                                %assuming arbitrary x20

t = length(Current);

Ib.signals.values = Current;
Ib.time = 1:t;
Ib.signals.dimensions = 1;

V.signals.values = Voltage;
V.time = 1:t;
V.signals.dimensions = 1;
```

Fig. 3.5.1 M-file code

The presented program enables reading the measured values of Voltage and Current as a files saved by the BMU. The data gathered by the measurement unit is saved as csv file, which is then read by Matlab using "fopen" command. The "textscan" command used in the fifth line separates the gathered data into different columns. Measured values of the Voltage and Current are assigned to the AvgCurrent and AvgVoltage arrays. Afterwards, two loops are created in order to clear the data of the invalid values added by Matlab in the process of reading the file. The x_{20} parameter is then initialized with an arbitrary value, which in this case is equal to 3. Lastly, values of the Current and Voltage are saved as a "structure with time" (structure consisting of a values vector and a time vector) for further use in the model.

The model created in the Simulink is presented in the figure 3.5.2.

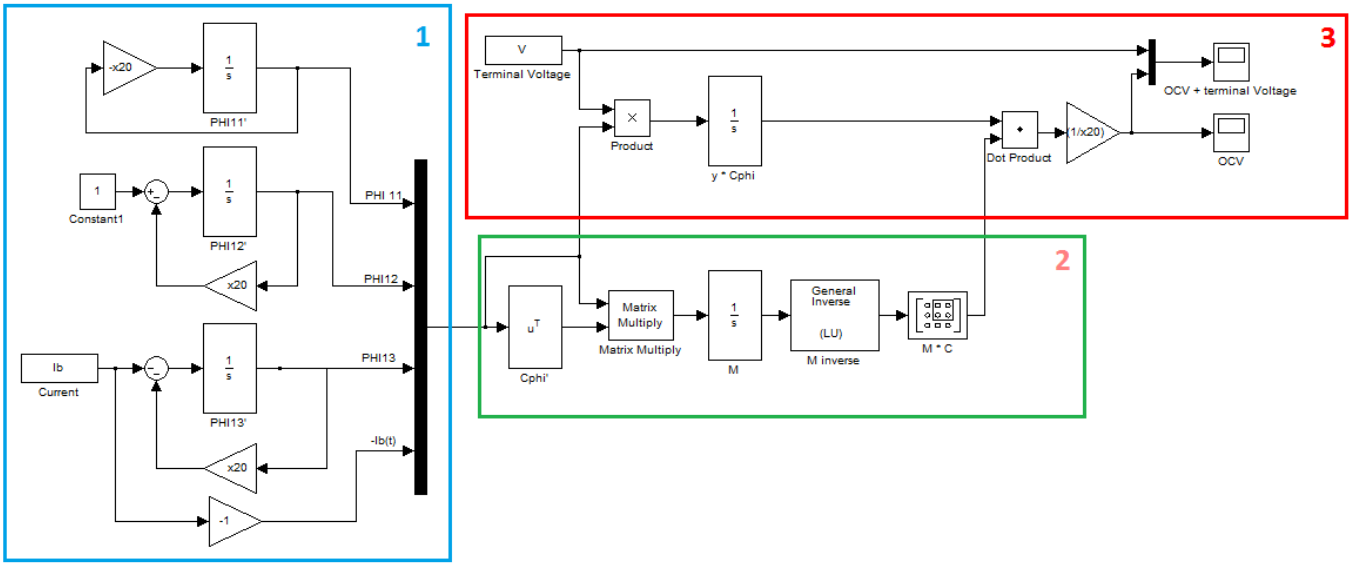

Fig. 3.5.2 OCV estimation method model

In the first part of the model (highlighted with the blue border) the derivatives of $I|$ are computed according to the equations (11) – (13). For reading convenience the mentioned equations are presented once again:

$$\frac{d\Phi_{11}}{dt} = -\Phi_{11}x_{20} \tag{11}$$

$$\frac{d\Phi_{12}}{dt} = -\Phi_{12}x_{20} + 1 \tag{12}$$

$$\frac{d\Phi_{13}}{dt} = -\Phi_{13}x_{20} - I_b(t) \tag{13}$$

The value of the x_{20} parameter is constant and equal to 3. It is observed that only $I|_{13}$ is time variant as the derivative depends on the terminal current. In order for the model to work it is necessary to run the script, prepared in the m-file presented in the figure 3.5.1 as the measured values of voltage and current must be loaded into the workspace. It is also imperative to set proper simulation time, equal to the length of time vectors of I_b and V structures. In the section 3.2 "Reference method" it was stated that the intercepts of the I_b fit to a quadratic equation (16)

$$I_b(t) = a + b(t - t_0) + c(t - t_0)^2 \tag{16}$$

should be used, however, practical implementation in Matlab environment allows for use of the terminal voltage and current trajectories. The "Current" and "Voltage" blocks allow for use of Ib and V variables from the workspace. One value from the vectors is used for each simulation step in the Simulink. The "mux" block represented as black filled rectangle creates a vector from the values of PHI11, PHI12, PHI13 and Ib(t) in the form:

$$\begin{bmatrix} \phi_{11} & \phi_{12} & \phi_{13} & -I_b(t) \end{bmatrix} = \phi(t) * C(t)$$

Where:

$$C(t) = \begin{bmatrix} 1 & 0 & 0 & -I_b(t) \end{bmatrix}$$

Second section of the model calculates matrix M, its inverse and multiplication with matrix C. Firstly, a transposed matrix of $I|(t) * C(t)$ was created using the "transpose" block from the DSP toolbox. Secondly, the aforementioned matrix was multiplied with its transposed version which in result created a matrix in the form of:

$$\phi(t)^T C^T \phi(t) C = \begin{bmatrix} \phi_{11}^2 & \phi_{11}\phi_{12} & \phi_{11}\phi_{13} & -\phi_{11} I_b(t) \\ \phi_{12}\phi_{11} & \phi_{12}^2 & \phi_{12}\phi_{13} & -\phi_{12} I_b(t) \\ \phi_{13}\phi_{11} & \phi_{13}\phi_{12} & \phi_{13}^2 & -\phi_{13} I_b(t) \\ -I_b(t)\phi_{11} & -I_b(t)\phi_{12} & -I_b(t)\phi_{13} & I_b(t) \end{bmatrix}$$

Thirdly, the matrix was integrated on the (t_0,t_f) period, which is the simulation time of the model. As a result the M matrix was created, which form is:

$$M(t) = \int_{t_0}^{t_f} \begin{bmatrix} \phi_{11}^2 & \phi_{11}\phi_{12} & \phi_{11}\phi_{13} & -\phi_{11}I_b(t) \\ \phi_{12}\phi_{11} & \phi_{12}^2 & \phi_{12}\phi_{13} & -\phi_{12}I_b(t) \\ \phi_{13}\phi_{11} & \phi_{13}\phi_{12} & \phi_{13}^2 & -\phi_{13}I_b(t) \\ -I_b(t)\phi_{11} & -I_b(t)\phi_{12} & -I_b(t)\phi_{13} & I_b(t) \end{bmatrix}$$

Lastly, the M matrix was inversed and multiplied by C in preparation to calculate OCV which was done in the third section. The inversion of the matrix was done through the use of "General Inverse" block from the "Matrix Inverses subsystem" available in the DSP toolbox. Multiplication of the M and C matrixes was done with the use of submatrix block which derives the second row of the M matrix, which is the result of the mentioned operation

The third and last section of the model calculates the OCV based on the equation (17).

$$V_{OC} = \lim_{t_f - t_0 \to \infty} \left(\frac{1}{x_{20}} * [0\ 1\ 0\ 0] M^{-1}(t) * \int_{t_0}^{t_f} \Phi^T(t) * C^T(t) * y(t) dt \right) \quad (17)$$

Firstly, the multiplication of the system's output (terminal voltage) with the $I|(t) * C(t)$ matrix is calculated. Afterwards, the result is integrated over the simulation time (t0,tf) which is equal to the length of the Current vector. The result of the aforementioned operations is a [1x4] vector. The "Dot Product" block multiplies two vectors element by element. Through the multiplication of the [1x4] and [4x1] vectors we receive a [1x1] vector as the output of the block. Lastly, the "Gain" block is used to multiply the result with a constant equal to $\frac{1}{x_{20}}$. The OCV curve created by the model can be viewed in the "Scope" blocks. The results of the presented method and comparison with the designed one will be shown in the section 4, "Tests".

3.5.2. Designed Algorithm MatLab Implementation

The algorithm's first cycle requires only one input from the user - the nominal capacity in Ah. All the other parameters, including the nominal voltage and battery behavior after disconnecting from a load (T1, T2 and T3 times) are counted by the algorithm. The first cycle also counts the temperature in which the battery is operating in order to make necessary voltage readings corrections. The first part of the MatLab m-file, which represents the first operation cycle is presented in the figure 3.5.3.

```
clear;
clc;

%% Load File, for simulation purposes only

f=fopen('ocvevery20.csv', 'rt');
C=textscan(f,'%f %s %f %f %s %f %s %s %f %s', 'delimiter' ,';', 'Headerlines', '1');
fclose(f);

AvgCurrent=C{1,3};
AvgVoltage=C{1,4};
AvgTemperature=C{1,1};
a=size(AvgCurrent);
j=1;
NominalCapacity=240;

for i=1:a(1,1)
    if mod(i,2)==1
        Current(j,1)=abs(AvgCurrent(i,1));
        if Current(j,1)>0 && Current(j,1)<0.11
           Current(j,1)=0;
        end
        j=j+1;
    end
end

j=1;

for i=1:a(1,1)
    if mod(i,2)==1
        Voltage(j,1)=AvgVoltage(i,1);
        j=j+1;
    end
end

j=1;

for i=1:a(1,1)
    if mod(i,2)==1
        Temperature(j,1)=AvgTemperature(i,1);
        j=j+1;
    end
end

```

Fig. 3.5.3 First cycle of the algorithm's operation (1/3)

Presented part of the code opens the pre-saved .csv (comma separated values) files, saved by Micropower's BMU and transfers the Current, Voltage and Temperature data into the MatLab workspace. The second part of the file is presented in the figure 3.5.4.

```
%% Detect the battery type (Nominal Voltage, OCV/SOC Characteristic)

if min(Voltage)>1.4 && max(Voltage)<2.5          %1 cell, 2V battery
    multiply=1;
elseif min(Voltage)>5 && max(Voltage)<7          %3 cells, 6V battery
    multiply=3;
elseif min(Voltage)>10 && max(Voltage)<14        %6 cells, 12V battery
    multiply=6;
elseif min(Voltage)>20 && max(Voltage)<28        %12 cells, 24V battery
    multiply=12;
elseif min(Voltage)>32 && max(Voltage)<40        %18 cells, 36V battery
    multiply=18;
end

%% Check the temperature of the battery operations, change the OCV/SOC
% characteristics accordingly

if min(Temperature)>69 && max(Temperature)<75
    add=0.032;
elseif min(Temperature)>63 && max(Temperature)<=69
    add=0.028;
elseif min(Temperature)>58 && max(Temperature)<=63
    add=0.024;
elseif min(Temperature)>52 && max(Temperature)<=58
    add=0.02;
elseif min(Temperature)>46 && max(Temperature)<=52
    add=0.016;
elseif min(Temperature)>40 && max(Temperature)<=46
    add=0.012;
elseif min(Temperature)>35 && max(Temperature)<=40
    add=0.008;
elseif min(Temperature)>29 && max(Temperature)<=35
    add=0.004;
elseif min(Temperature)>20 && max(Temperature)<=29
    add=0;
elseif min(Temperature)>14 && max(Temperature)<=20
    add=-0.004;
elseif min(Temperature)>6 && max(Temperature)<=14
    add=-0.008;
elseif min(Temperature)>2 && max(Temperature)<=6
    add=-0.012;
elseif min(Temperature)>-3 && max(Temperature)<=2
    add=-0.016;
elseif min(Temperature)>-9 && max(Temperature)<=-3
    add=-0.02;
elseif min(Temperature)>-15 && max(Temperature)<=-9
    add=-0.024;
elseif min(Temperature)>-20 && max(Temperature)<=-15
    add=-0.028;
```

Fig. 3.5.4 First cycle of the algorithm's operation (2/3)

In the second part of the file, algorithm checks the minimum and maximum voltage measurements, fitting it's values into one of the most common cell configurations, i.e. 2V, 6V, 12V, 24V and 36V batteries. Apart from the Nominal Voltage, the operating temperature is checked. Depending on the temperature of a battery, certain offset must be added to the

voltage readings. The temperature / voltage change relation for the Wet Cell Lead-Acid batteries according to The Battery Council [14] is presented in the table 3.1. The operating temperature of a battery is a critical factor and should always be included in the SOC estimation, ex. Between 70°C and 10° C the open circuit voltage reading differs by 0,26, translated to the OCV/SOC relationship not including the temperature difference produces around 40% error in SOC estimation.

Temperature (°C)	Voltage add (12V)	Voltage add (2V)
71.1°	0,192	0,032
65.6°	0,168	0,028
60.0°	0,144	0,024
54.4°	0,12	0,02
48.9°	0,096	0,016
43.3°	0,072	0,012
37.8°	0,048	0,008
32.2°	0,024	0,004
26.7°	0	0
21.1°	-0,024	-0,004
15.6°	-0,048	-0,008
10°	-0,072	-0,012
4.4°	-0,096	-0,016
-1.1°	-0,12	-0,02
-6.7°	-0,144	-0,024
-12.2°	-0,168	-0,028
-17.8°	-0,192	-0,032

Tab. 3.1 Temperature/ voltage modification relationship for Flooded Lead-Acid batteries

Temperature of the cell varied between 20 and 22 °C throughout the whole testing phase. However, the code above includes the possible temperature changes as a voltage readings adjustment, ex. if the battery operated in 44 degrees the 0.012 V would be added per cell to the readings, affecting the OCV/SOC graph. The third part of the file is presented in the figure 3.5.5.

In this part of the file, the OCV/SOC graph is prepared according to the Nominal Voltage and Temperature readings. The variable "multiply" is produced by the voltage check if-loop and the "add" is produced by the temperature check if-loop. All together the algorithm detects the nominal voltage and battery internal temperature and produces an OCV/SOC graph accordingly. Apart from this, the third part of the m-file reads the first cycle data, including the long rest period in order to find the T1, T2, T3 time. It describes the battery

dynamics and the "Diff1" and "Diff2" - Voltage differences between the T3 and T1, T3 and T2, which enabled the voltage estimation for "Semi-OCV" periods.

```
t=0.1:0.1:1;
OCVx=0.1:0.01:1;
p=multiply*(add+[1.9500 1.9733 1.9900 2.0100 2.0300 2.0533 2.0700 2.0900 2.1067 2.1267]);
OCVy=interp1(t,p,OCVx,'spline');
figure(1);
plot(t,p,'o',OCVx,OCVy)


%% Find the T1, T2 and T3 times, calculate the Voltage differences at those
% points (diff1, diff2)

R1=0;
R2=0;
R3=0;
R4=0;

for i=1:length(Current);

    if  Current(i,1)==0 && R3==0    %% if put on hold and T3 was not found
        if R4==0
           T0=i;
           R4=1;
        end
        if i>31
           if Voltage(i)==Voltage(i-30) && R1==0
           T1=i-30-T0;
           R1=1;
           end
        end
        if i>151
        if Voltage(i)==Voltage(i-150) && R2==0
            T2=i-150-T0;
            R2=1;
        end
        end
        if i>2701
        if Voltage(i)==Voltage(i-2700) && R3==0
            T3=i-2700-T0;
            R3=1;
        end
        end
    end
end

Diff1=Voltage(T0+T3)-Voltage(T0+T1);         %estimated difference between voltage in T1 and T3 (OCV)
Diff2=Voltage(T0+T3)-Voltage(T0+T2);         %estimated difference between voltage in T2 and T3 (OCV)
```

Fig. 3.5.5 First cycle of the algorithm's operation (3/3)

OCV/SOC graph, produced for the 6V battery in 20 °C is included in the figure 3.5.6. The OCV/SOC relationship was found as a technical brochure of Fullriver Batteries company [15]. This relationship is a basis for counting an error between the Coulomb Counting and OCV Lookup methods, consequently leading to calculation of the correction factor, by which the current is multiplied in order to increase/decrease the changes in integrated Ampere-hours. It is crucial to make sure that the used OCV/SOC relationship graph suits the used battery type and is valid, before starting the algorithm. Between the Wet cell, AGM and Gel cell batteries there is a significant difference in OCV/SOC relation, mostly because of different life-cycles and capacities. Also the battery quality affects the OCV/SOC relation. Therefore it

is recommended to ensure that we use the proper producer's documentation before we use the algorithm.

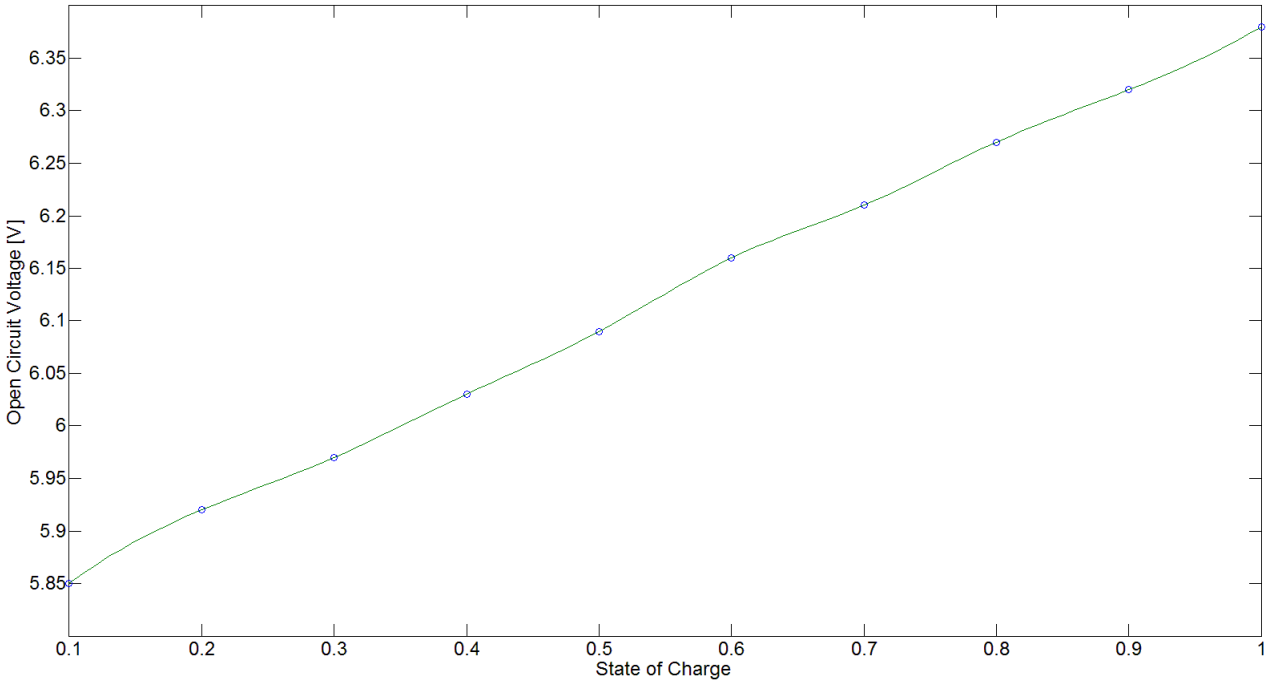

Fig. 3.5.6 OCV/SOC relationship for the 6V battery, working in 20 °C

Due to the need of simulating the real-time battery cycle, the main part of the algorithm was created and implemented in MatLab Simulink software. The overview of the Simulink program is presented in the figure 3.5.7.

The program can be divided into 4 main parts (in colored borders - 1.green, 2.red, 3.blue, 4.yellow). Each part will be described below with the insight into subsystems and graphs, output examples and description of the role and significance of each block.

- First Part (1, green border) - responsible for unmodified coulomb counting of a current, detecting the T1, T2 and T3 points in the present current characteristics and creating the estimated OCV graph.
- Second Part (2, red border) - the Error counter is implemented in this part, using the T1-T3, Voltage, Current, SOC (Ah) and SOC (Ah modified with factor). It compares the SOC, giving the error value and then translates it into Ah number to be added within the next hour of the discharge.
- Third part (3, blue border) - includes pure algebraic operations of counting the correction factor and deciding when it should be multiplied by the actual current

- Fourth part (4, yellow border) - acts as a modified Ah counter, closing the feedback loop of a modified SOC value with reduced error.

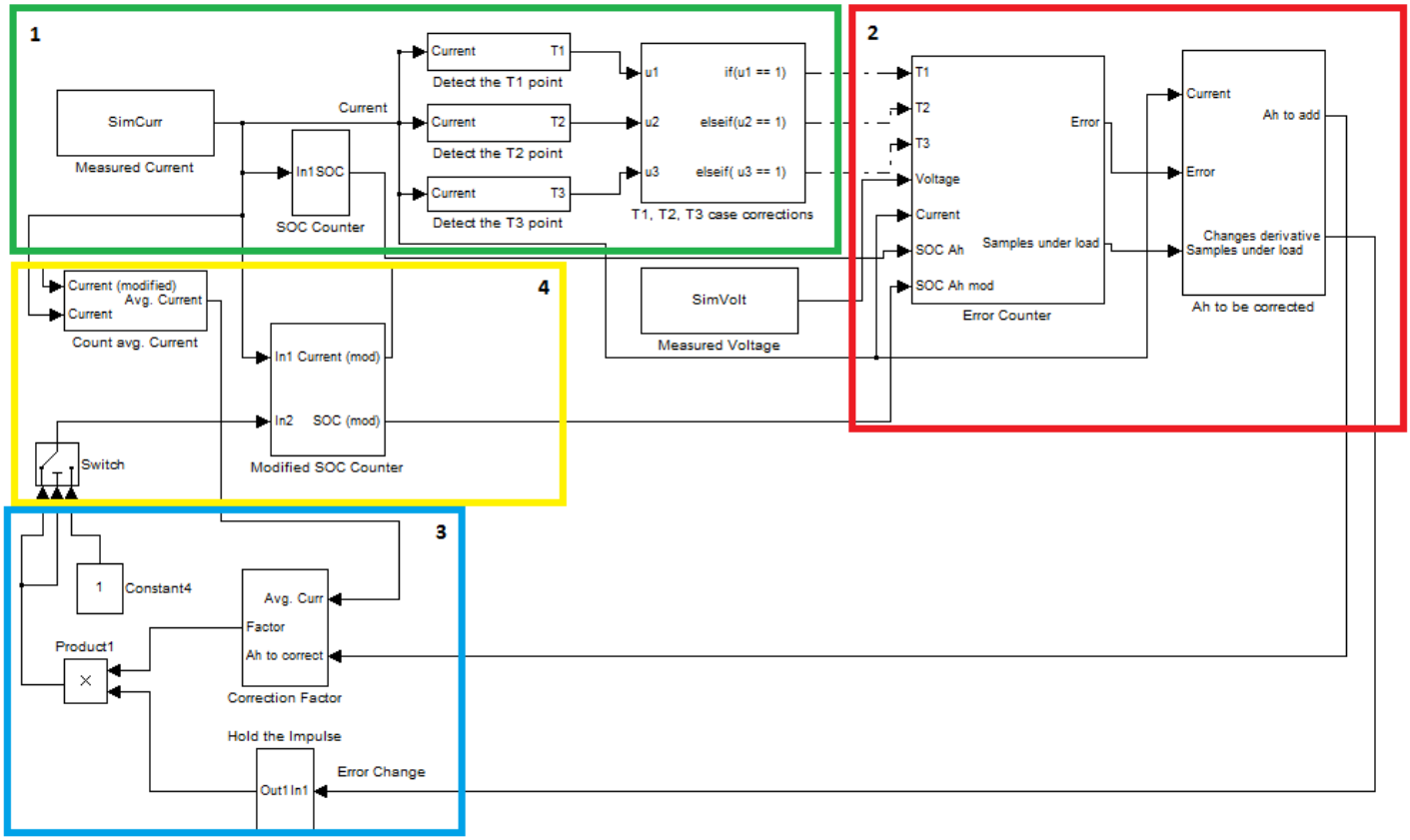

Fig. 3.5.7 Overview of the algorithm in MatLab Simulink.

In order to make the program logic more understandable, each subsystem will be opened, described and its output presented, along with all necessary comments on it in order to be re-implemented in any chosen programming language. Beginning with the first part (green) from the figure 3.5.7. - the "SOC Counter" block is presented in the figure 3.5.8.

The SOC Counter is a typical Coulomb Counter. Having a current value as an input, integrating it over time and dividing per 1800 (each sample is taken every 2 seconds of a real time, making 1800 samples equivalent of 3600 seconds, which is 1 hour) enables the algorithm to represent the number of Ampere-hours drawn from the battery. The next step is dividing this number by "Nominal Capacity" of a battery, which - in case of the new battery - is the operator's input as a number of Capacity (in Ampere-Hours, typically for C10 Discharging current). In the case of used battery it should be the State of Health multiplied by the Nominal Capacity. The output of the divide block is a Depth of Discharge, so it has to be subtracted from 1 to represent the State of Charge. The output value of this block is a SOC over time chart, example of which is presented in the figure 3.5.9.

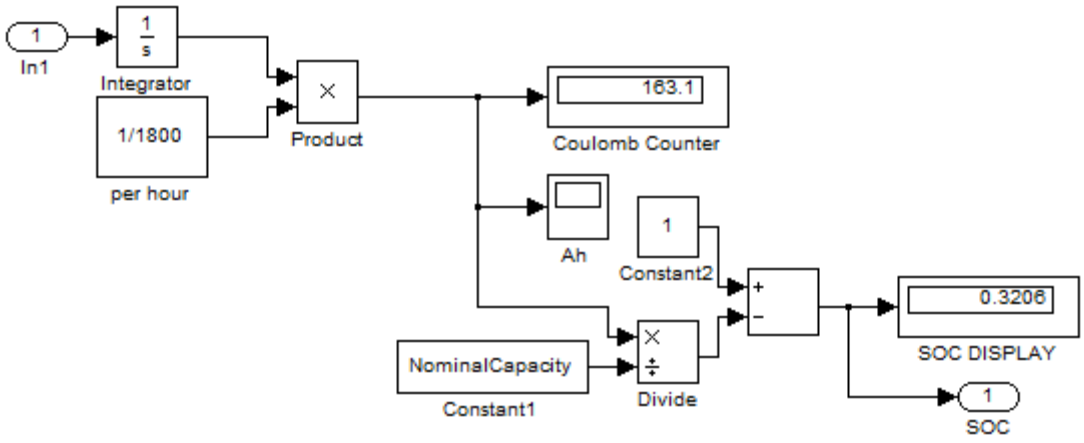

Fig. 3.5.8 "SOC Counter" block, responsible for coulomb counting.

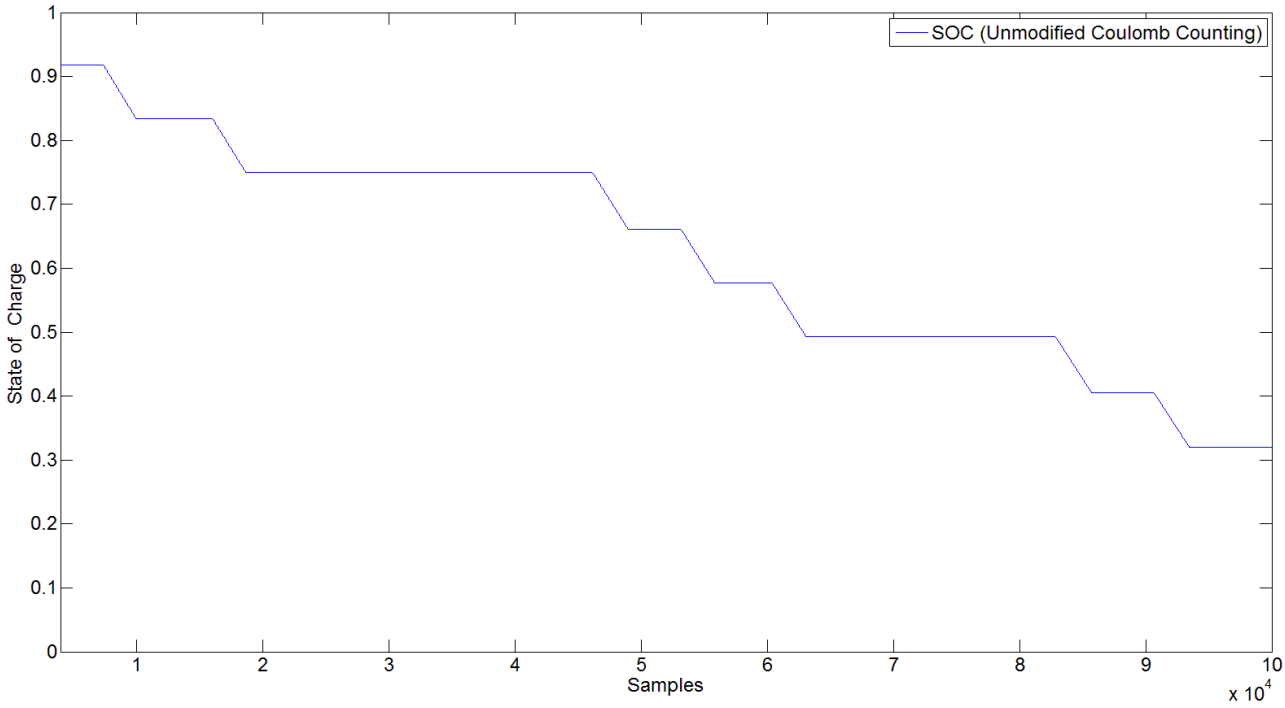

Fig. 3.5.9 Example of SOC Counter output graph - the SOC changes over time during the typical discharge.

The next part in the algorithm is formed as a series of 3 similar subsystems, called "Detect the Tx point". "Detect the T1 point" is pictured in the figure 3.5.10

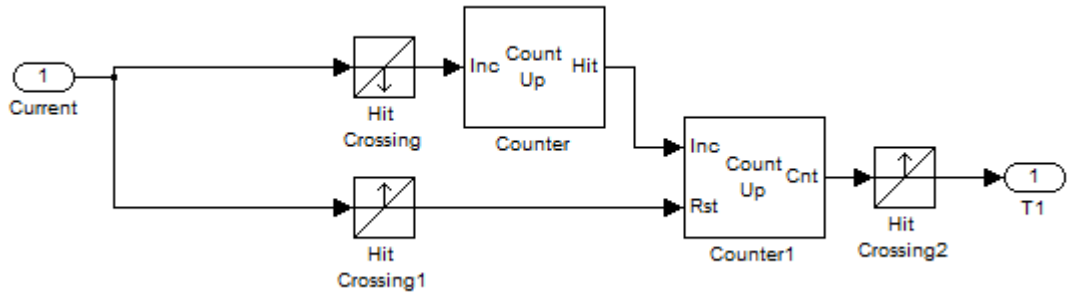

Fig. 3.5.10 "Detect the T1 point" block, responsible for detecting a time, in which all conditions for T1 to occur are satisfied and T1 estimate can be used as an OCV.

Each of the "Detect" blocks takes a value of the current as an input, checks if it hits 0 value from the top (if the battery was put on hold) then the counter is used to check if the time on hold reaches the T1 samples, in this case 74. If the current value is 0 for 74 samples the output of this block is a logical 1. "Detect the T2 point" and "Detect the T3 point" blocks work in the same manner, outputting 1 only at times when the battery is on hold for T2 or T3 time periods.

After this block series the IF/ELSE block called "T1, T2, T3 Case corrections" is presented, giving the priority of T3 over T2 and T2 over T1. Prioritizing the most precise (T3) OCV value over the less precise (T2, T1) OCV estimates, outputting the most precise estimation. Ex. when the battery is put on hold for a certain time, reaching T2, but not enough for T3, the system will prioritize the T2 output over the T1 output, knowing that T2 estimate is more precise than T1.

The second part (red border) of the algorithm includes the most important computations. The "Error Counter" Block is presented in the figure 3.5.11. The block has 7 inputs, out of which two are measured and 5 are counted or estimated by the algorithm. First of all, depending on the active Tx, voltage value is summed with the "diff" parameter or stays without a change. Ex. if T3 is active (the certain time passed after the battery was put on hold) nothing is added to the original voltage (it is assumed that this value is an actual OCV). On the other hand If only T1 is active the "Diff1" parameter is added to the measured voltage, forming an OCV estimate.

The estimated OCV value is then translated into the SOC according to the OCV/SOC lookup table (an example may be found in the figure 3.5.6). Afterwards, it is compared to the counted Ampere-hours sum (an output from the modified coulomb counting block), forming an error value to be corrected in the next hour of the battery discharge.

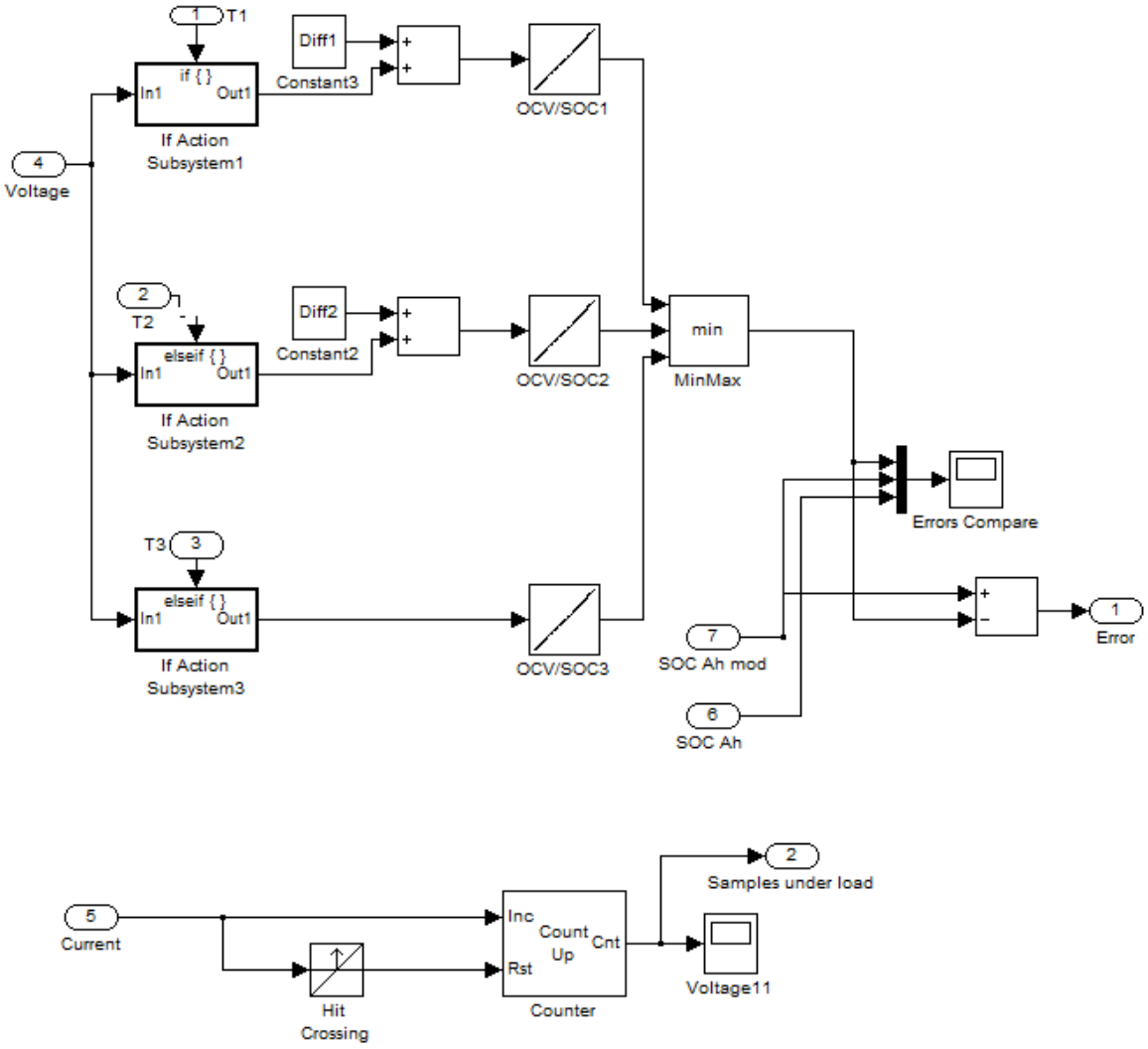

Fig. 3.5.11 "Error Counter" block, responsible for comparing the SOC counted by coulomb counter and the more precise - SOC counted by translating OCV to SOC.

To give a better insight into the "Error Counter" operations, an example of its output is presented as a graph in the figure 3.5.12. Although the graph is drawn continuously, only few of the values (highlighted with the red circles) are taken into consideration by the algorithm. Note that the variable part of the graph pictures the moments, in which the current is being drawn, i.e. all three T1, T2 and T3 times are inactive and thus there is no way to estimate the OCV. At those times, the previously counted correction factor is active, affecting the error from the last discharge period. The error value will be discussed more deeply, along the rest of the results in the next chapter.

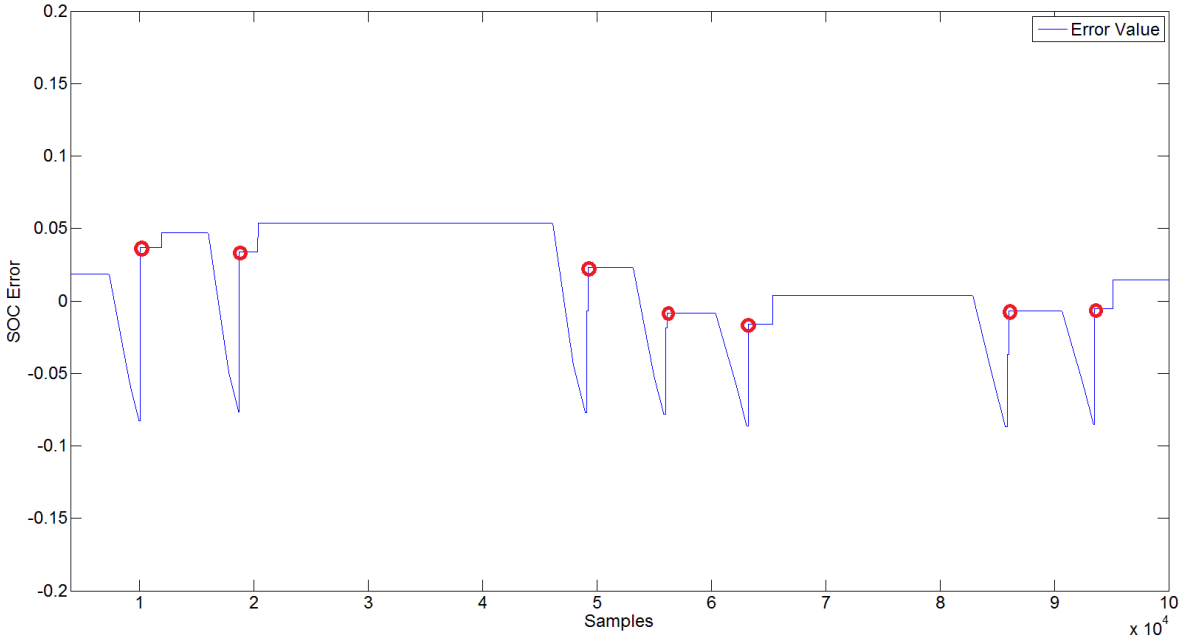

Fig. 3.5.12 Example of "Error Counter" output, valid error values are highlighted with the red circles.

The next block, called "Ah to be corrected" is presented in the figure 3.5.13.

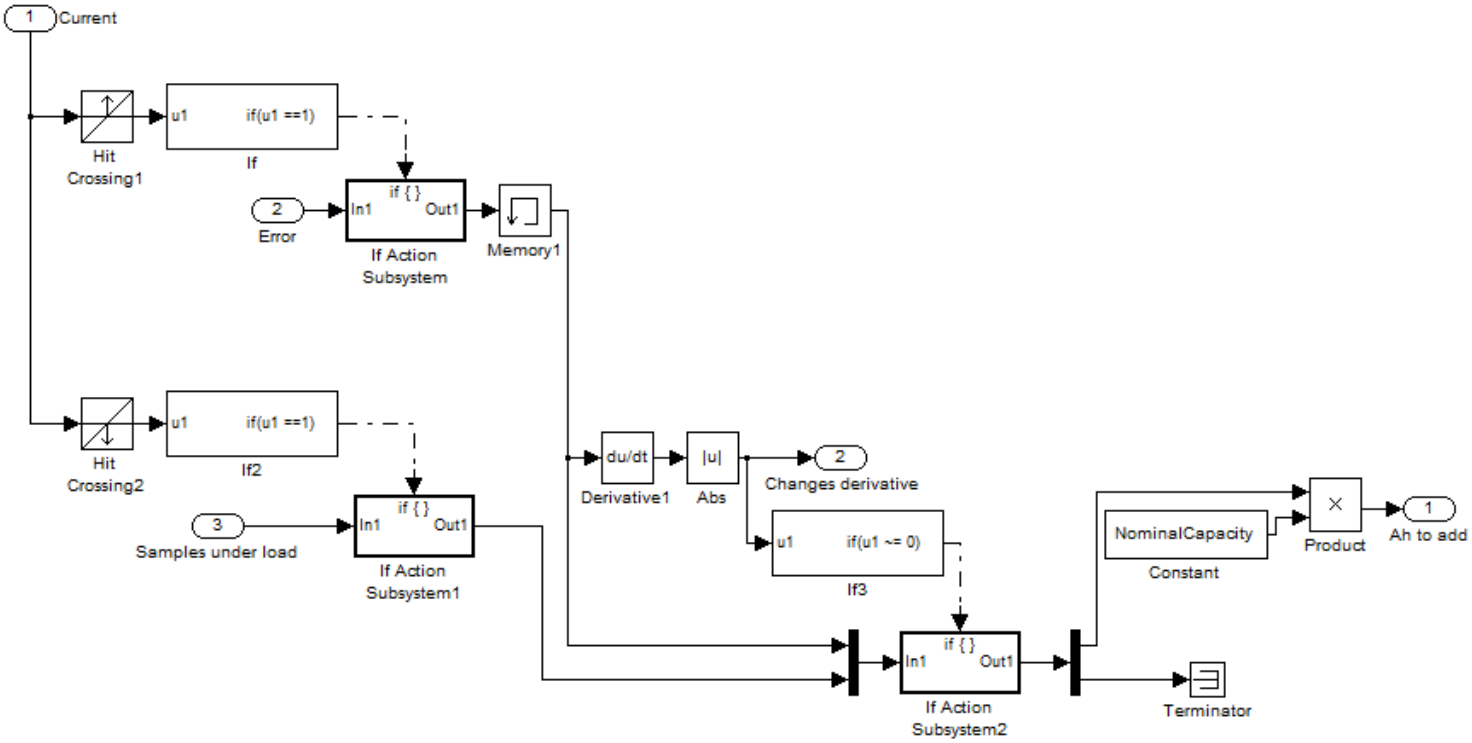

Fig. 3.5.13 "Ah to be corrected" block, responsible for translating the "Error" value

The block is designed to detect moments when another discharge starts, save the counted error values in those times and check when the error values actually changes (after each discharge). The example of the output of this block is presented in the figure 3.5.14.

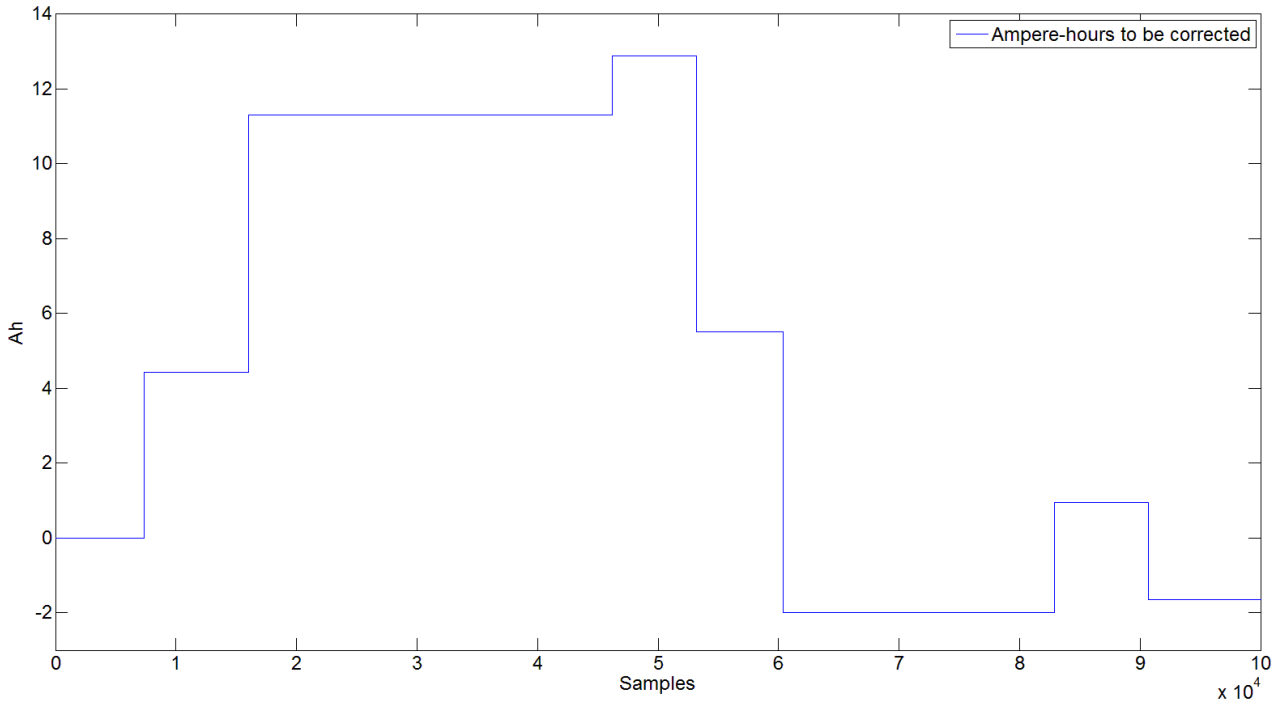

Fig. 3.5.14 Output from the block "Ah to be corrected", an error translated into Ampere-Hours to be modified in the next discharge phase.

The block outputs the Ampere-Hours number, however, it is crucial that it outputs the number in the right time. Using double “if” loop it is designed to start new counting only when the error derivative is positive, i.e. only when error changes.

The first block from the third (blue border) part of the algorithm is called "Hold the Impulse" and its internal structure is presented in the figure 3.5.15. This block has the absolute value of the current derivative as an input. Its aim is to hold the impulse for one hour, giving 1 as an output at the times the algorithm detects start of the next discharge period and 0 at all other times. The output of this block will be multiplied with the correction factor value in the next step, forming an actual correction factor affecting the real coulomb counter only at a certain times. The example of the output from this block is presented in the figure 3.5.16.

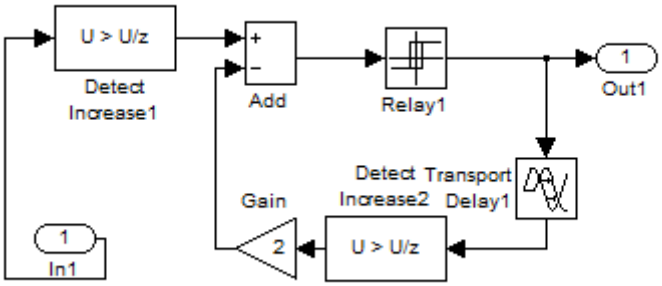

Fig. 3.5.15 "Hold the Impulse" block, used to detect the impulse of error's change and hold it from another discharge start for one hour.

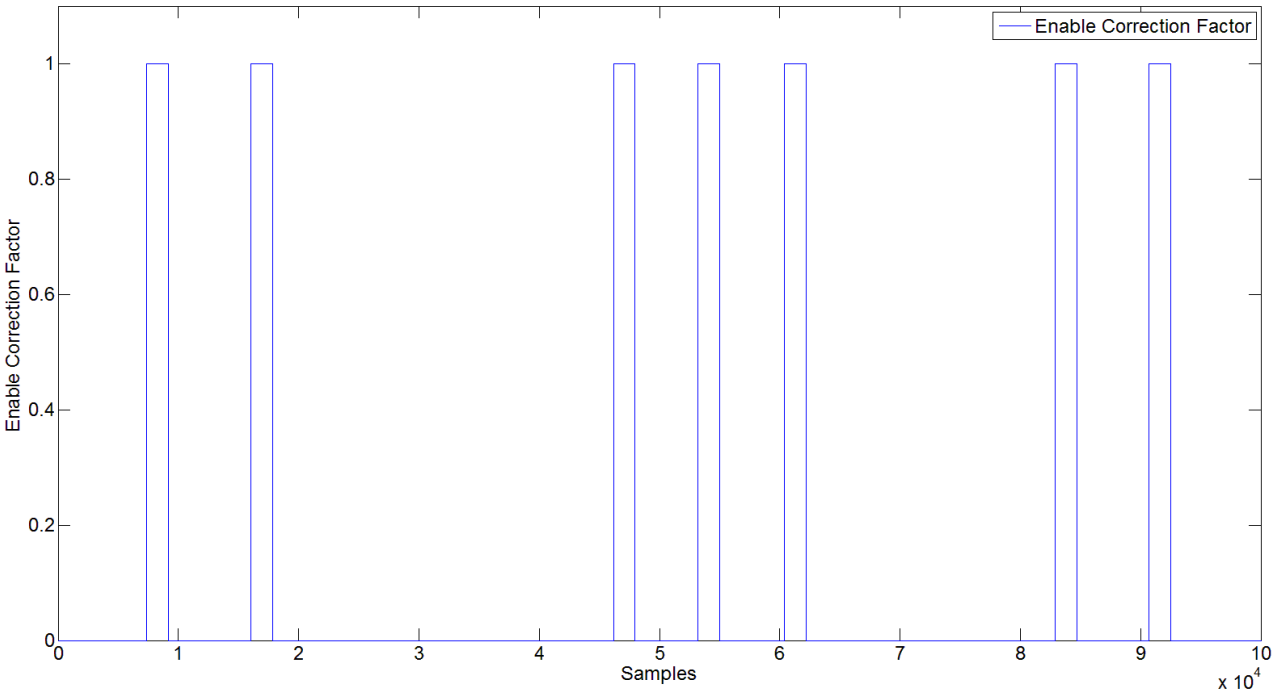

Fig. 3.5.16 Example of an output from the "Hold the Impulse" block

As may be seen above, the impulses are held for 1 hour - 1800 samples from the impulse, denoting the start of another discharge phase. The block parallel to this one is called "Correction Factor" and must not be underestimated. It translates the "Ah to be corrected" output into the actual factor, by which the current value should be multiplied in order to reduce the coulomb counting error. The internal structure of the "Correction Factor" block is presented in the figure 3.5.17. Its purpose is a practical realization of the previously mentioned Correction Factor equation by dividing the sum of Ah to be corrected and the Average Current by the Average Current itself. The factor has values of over 1 if there is a

need to speed up the coulomb counting (the error is positive) and the values below 1 if there is a need to slow down the counter (the error is negative). Example of an output from this block is presented in the figure 3.5.18.

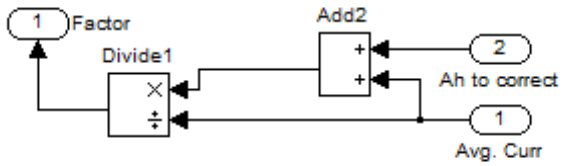

Fig. 3.5.17 "Correction Factor" block.

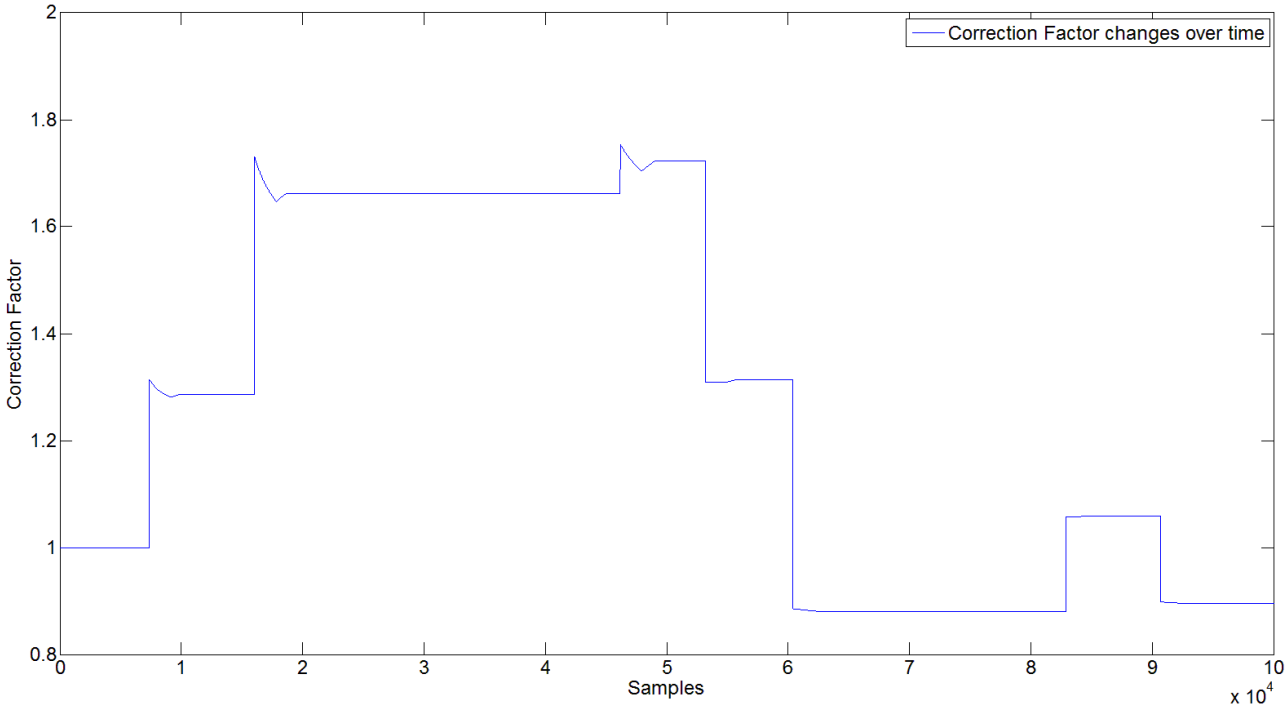

Fig. 3.5.18 Example of an output from the "Correction Factor" block.

The outputs from the previous 2 blocks are multiplied, forming a vector with the correct values of the Factor placed at correct times. Multiplied outputs are presented in the figure 3.5.19.

After this step, the factor is ready to be multiplied by the measured current value. The most important block from the fourth (yellow border) part of the algorithm is called "Modified SOC Counter". Its internal structure is presented in the figure 3.5.20. This block closes the feedback loop of an algorithm, forming next, corrected input (SOC value) for the

"Error Counter" block. The output from the "Modified SOC Counter", as the name says, is affected by corrections, which purpose is to reduce the error in the next discharge phases.

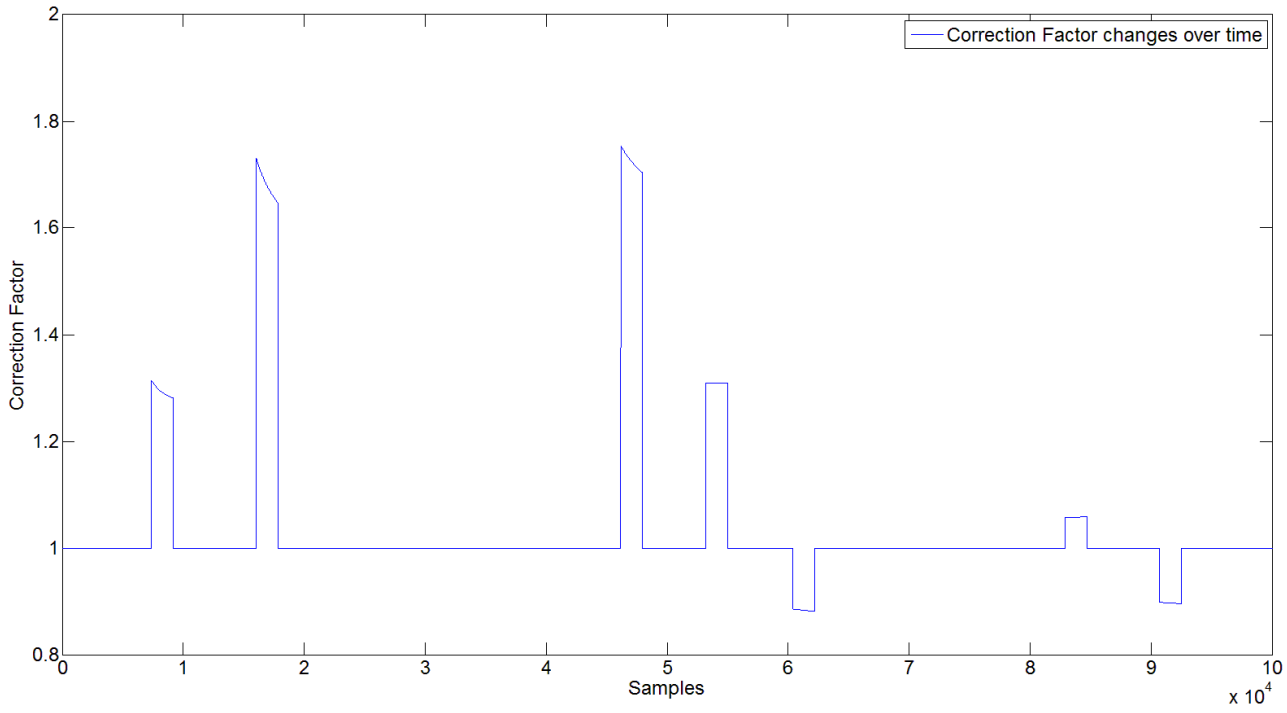

Fig. 3.5.19 Actual "Correction Factor" graph, the factors put in the proper discharge start times.

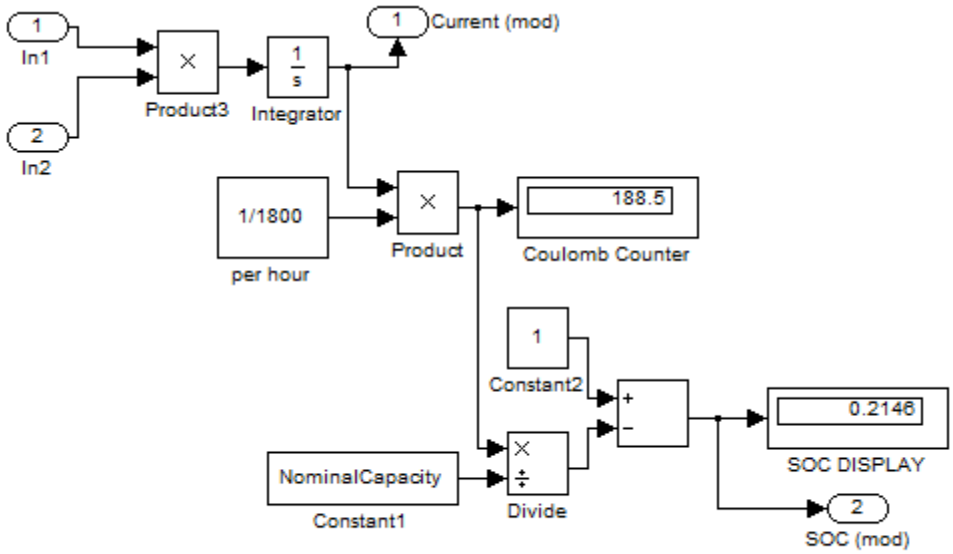

Fig. 3.5.20 "Modified SOC Counter" block, very similar to the "SOC Counter" block described before, but includes the Correction Factor.

The example of "Modified SOC Counter" output is presented in the figure 3.5.21.

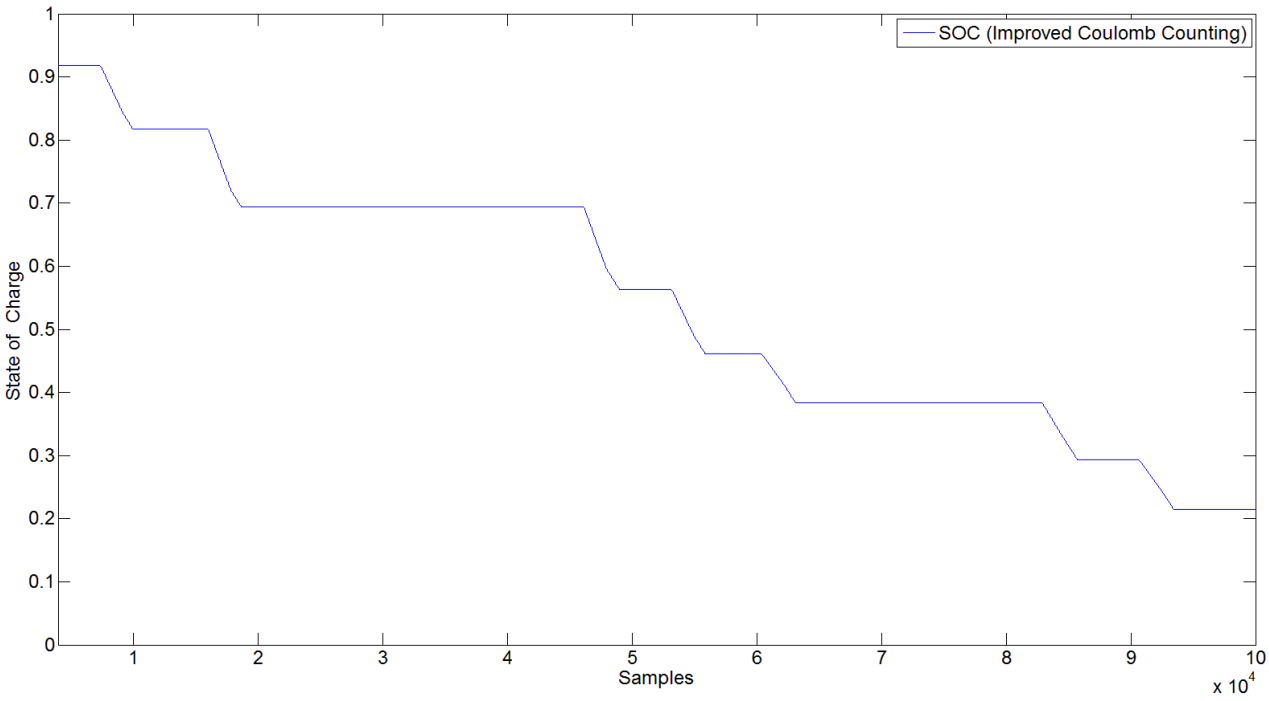

Fig. 3.5.21 Output from the "Modified SOC Counter" block, comparing to the "SOC Counter" block. The current values are visibly modified, causing the counter to accelerate or decelerate the counting.

This chapter will be concluded in chapter 4 "Tests" as all the results are presented there. Both program parts are attached to this Thesis in the same form as they appear in the paper.

3.5.3. SOH estimation

In this section a possible implementation of an SOH estimation technique will be presented. The designed method would greatly benefit from the addition of state of health estimation. In the current state the method uses nominal capacity of the battery in the calculations which will result in error increase in the long term use. The possible implementation will be presented as an integral part of the designed method. Firstly, a flowchart of the algorithm will be presented in figure 3.5.22:

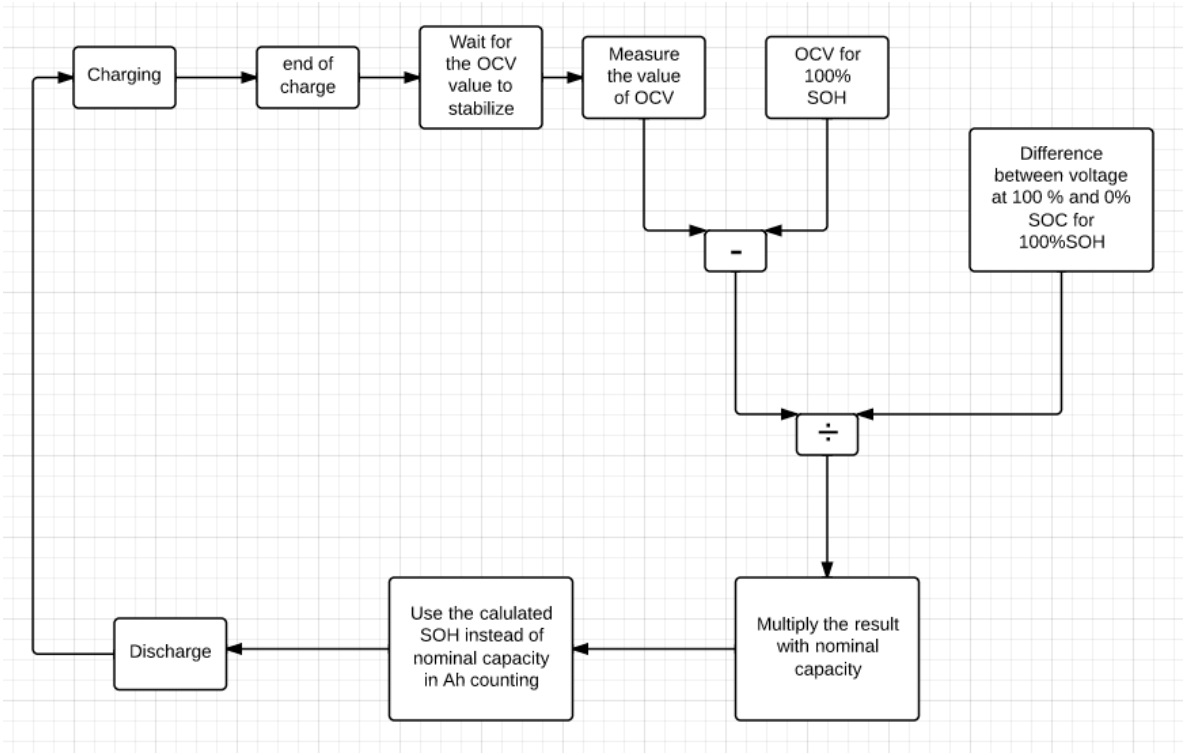

Fig. 3.5.22 The SOH estimation algorithm flowchart

The time it takes for the battery's terminal voltage to stabilize and reflect the open circuit voltage may vary depending on the battery type. In the project presented in this paper it is equal to 2 hours. Measured voltage is then subtracted by the OCV of a fully charged and at 100% SOH battery. In the case of 6V lead-acid battery the value is equal to 6.40 V. The difference of voltages at 100 % and 0% SOC for 100% SOH is calculated only once, at the first cycle. It is calculated based on the OCV/SOC curve presented and described in the section 3.5.1 in the figure 3.5.6. The division of the aforementioned values results in a SOH correction factor, which is then multiplied by nominal capacity. The calculated SOH value is then used in Ah counting, decreasing the error caused by aging effects of the battery.

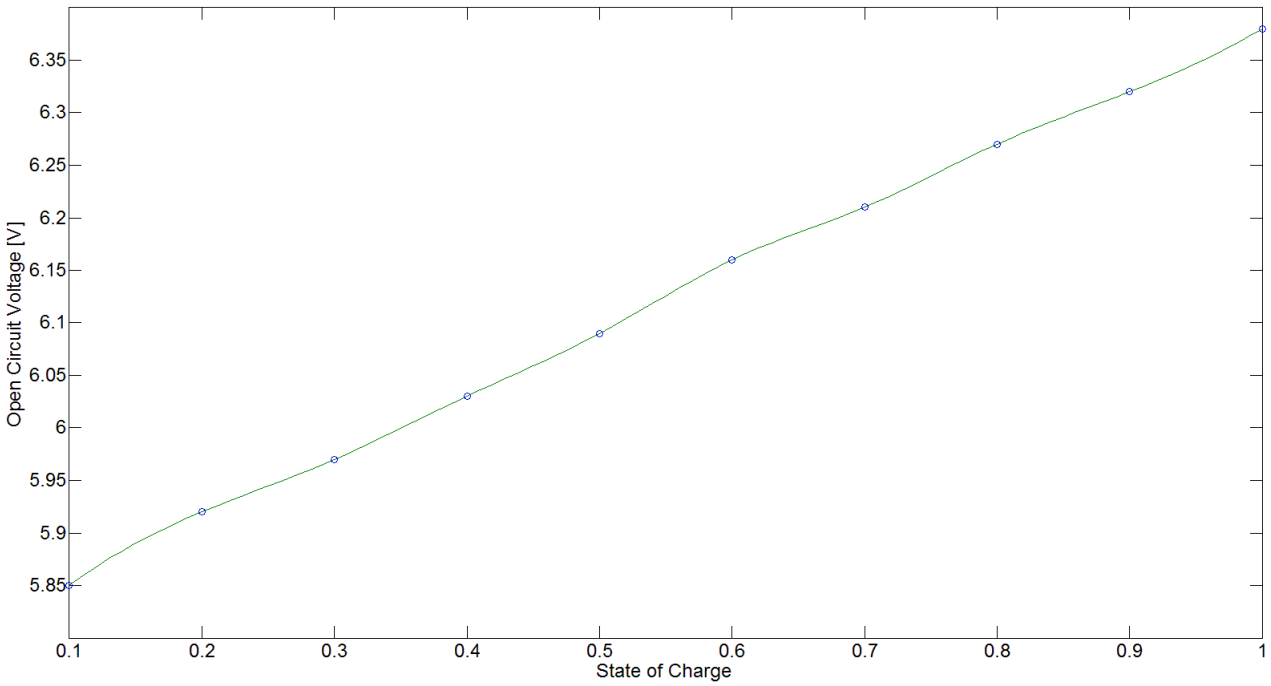

Fig. 3.5.6 OCV/SOC relationship for the 6V battery, working in 20 °C

It is important to note that the SOH algorithm will update only when the battery is fully charged after the discharge cycle. Moreover, the time required for the terminal voltage to reach the value of OCV may differ depending on the battery. However, if the aforementioned requirements are met, the presented method is a simple and effective solution. The presented SOH estimation method can also be easily fit into the designed method as all of the necessary variables are available. Possible implementation of the SOH estimation is presented in figure 3.5.23:

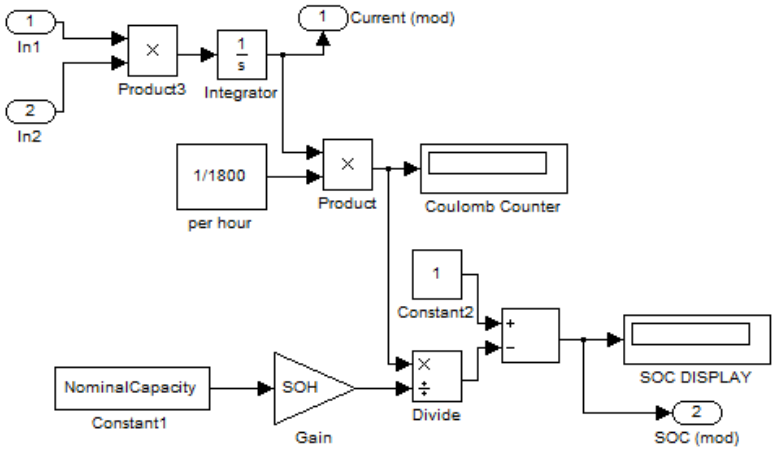

Fig. 3.5.23 "SOC Counter" block, responsible for coulomb counting with the improvement as a pre-counted gain SOH factor.

It is imperative to state that the SOH estimation is not implemented in the given project. The SOH "Gain" block would have the value of SOH correction factor calculated by the program according to the algorithm presented in the figure 3.5.22. In order to properly describe the suggested method an example will be shown with assumed values.

Assuming that the number of Ah counted is equal to 180:

The Coulomb counter has calculated that:

$$SOC = 1 - \frac{Counted\ Ah}{Nominal\ Capacity} = 1 - \frac{180}{240} = 0.25$$

However, the calculation was done after the 300th cycle and the maximum capacity of the battery is no longer 240 Ah. Let's assume that the measured OCV after charge is equal to 6.34 when the starting value was 6.38. As a result of this the error is equal to:

$$OCVerror = \frac{0.04}{6.38 - 5.85} = 0.075$$

Which means that the actual maximum capacity of the battery is equal to:

$$actual\ capacity = 240 - (240 * 0.0075) = 222Ah$$

If the SOH estimation method would be implemented and the algorithm would recognize the real value of maximum capacity is 222 the result would be:

$$SOCnew = 1 - \frac{Counted\ Ah}{actual\ capacity} = 1 - \frac{180}{222} = 0.19$$

It is observed that the difference in the calculated SOC is equal to 0.07 which may prove to be significant error. In the presented case the value of SOC would drop below 20, which would accelerate the battery's aging process. Such event would be highly undesirable by the user of the battery.

4. Tests

4.1. Reference method

In this subsection results of the tests conducted on the reference method will be presented. The current and voltage curves used for calculation of the OCV by the method are presented in the figures 4.1.1 and 4.1.2 respectively.

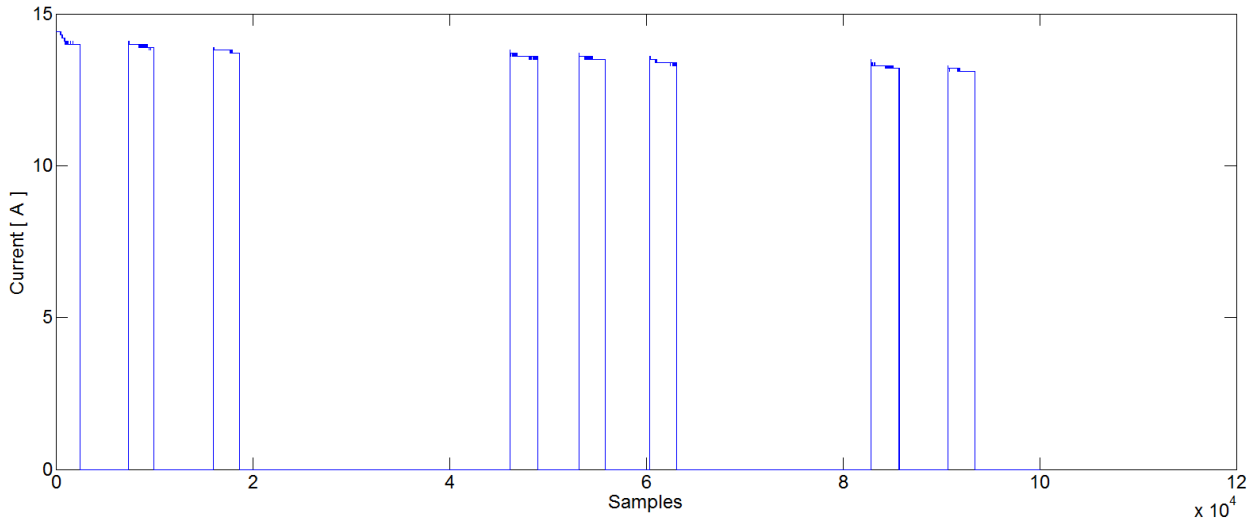

Fig. 4.1.1 Measured Current

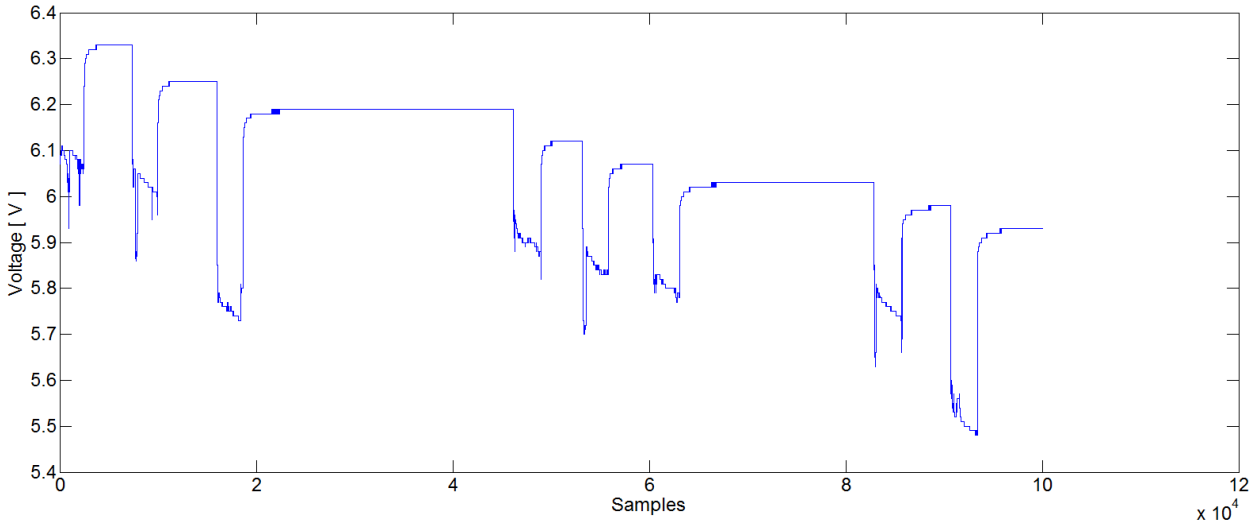

Fig. 4.1.2 Measured Voltage

In the figure 4.1.3 the calculated OCV in regard to terminal voltage is presented:

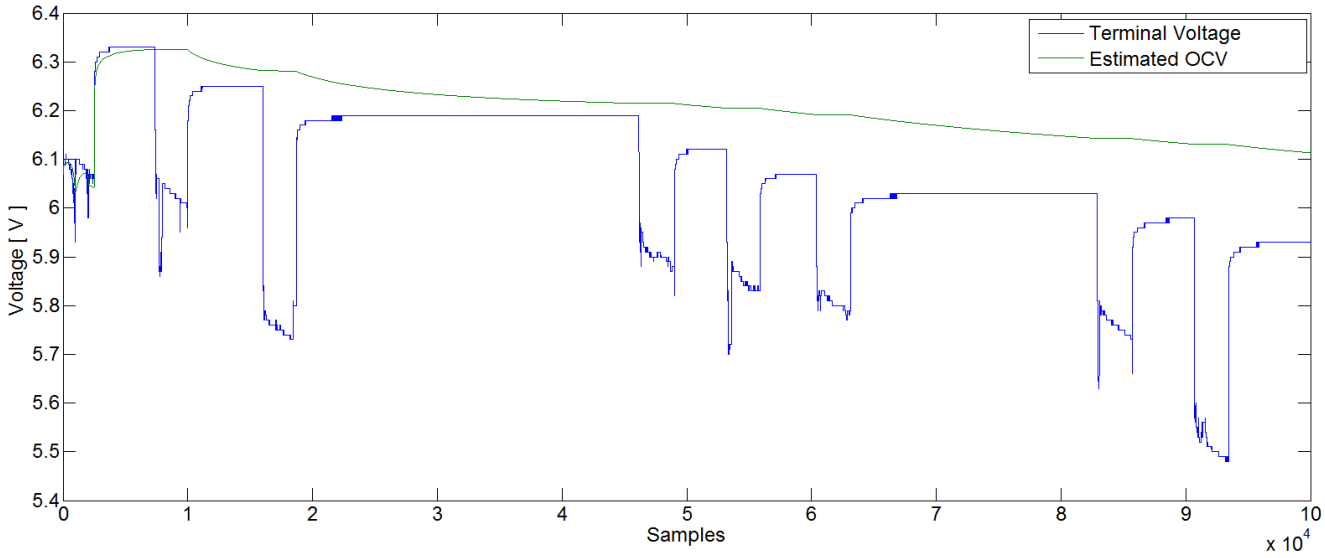

Fig. 4.1.3 Terminal voltage and calculated OCV

It is observed that the error in calculation of the OCV is increasing with the time. In order to properly explain the reasons behind such occurrence a few theoretical facts regarding the method must be brought. Firstly, the system in the form:

$$\frac{d}{dt}\begin{bmatrix} z_1(t)) \\ z_2(t)) \\ z_3(t)) \\ z_4(t)) \end{bmatrix} = \begin{bmatrix} -x_{20} & 1 & -I_b(t) & 0 \\ 0 & 0 & 0 & 0 \\ 0 & 0 & 0 & 0 \\ 0 & 0 & 0 & 0 \end{bmatrix} \begin{bmatrix} z_1(t)) \\ z_2(t)) \\ z_3(t)) \\ z_4(t)) \end{bmatrix}$$

$$z(t_0) = \begin{bmatrix} x_{10} \\ x_{20} \\ x_{30} \\ x_{40} \end{bmatrix} \quad y(t) = \begin{bmatrix} 1 & 0 & 0 & -I_b(t) \end{bmatrix} \begin{bmatrix} z_1(t) \\ z_2(t) \\ z_3(t) \\ z_4(t) \end{bmatrix}$$

is observable only when the current $I_b(t)$ is not constant. This phenomenon is observed in the presented figure, when the OCV remains at the same value for periods of time. During the period of 40 minutes after the current stopped flowing, the value of terminal voltage should be close to the real open circuit voltage. The measurements were taken every 2 seconds, which means that the 40 minutes equal ~1200 samples in the presented figure. It can be observed that the values of calculated OCV and terminal voltage after 1200 samples without current differ significantly. However, it is imperative to notice that in the article “Estimating the State of Charge of a Battery” by John Chiasson and Baskar Vairamohan it is stated that the method

requires resetting to work properly. It is also worth noting that presented in the paper experiments were carried out with much shorter times (1000 s).

Figures 4.1.4, 4.1.5 and 4.1.6 present the calculated OCV if the method is reset twice, at equal intervals of 33366 samples:

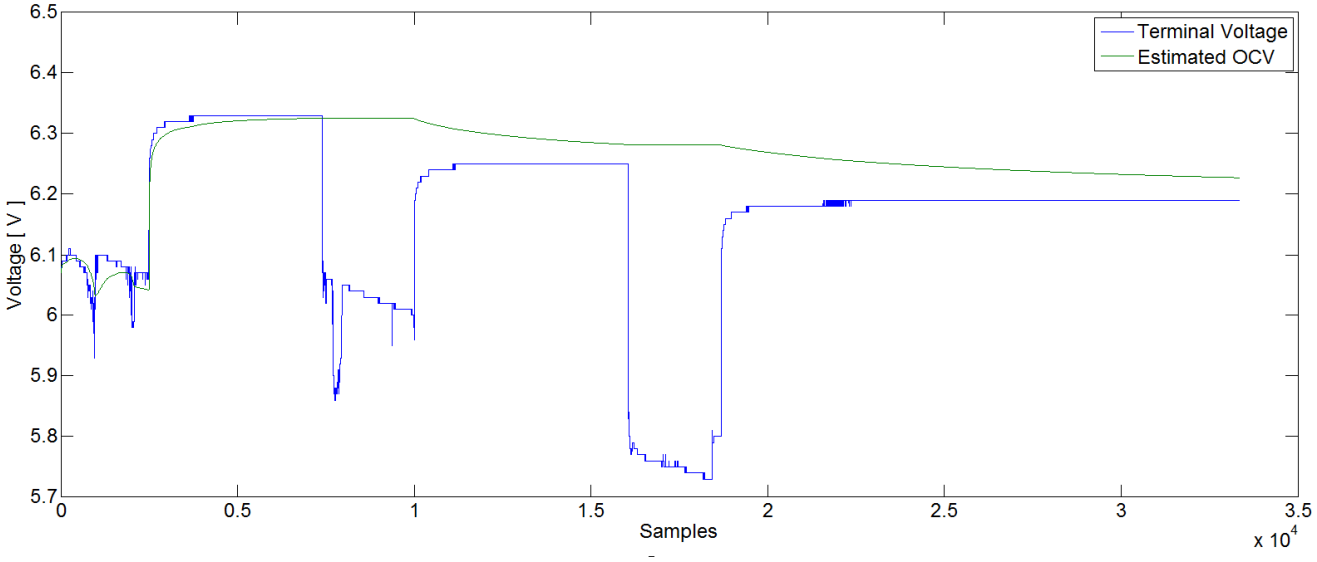

Fig. 4.1.4 Calculated OCV and terminal voltage in the first 33366 samplesFig. 4.1.5

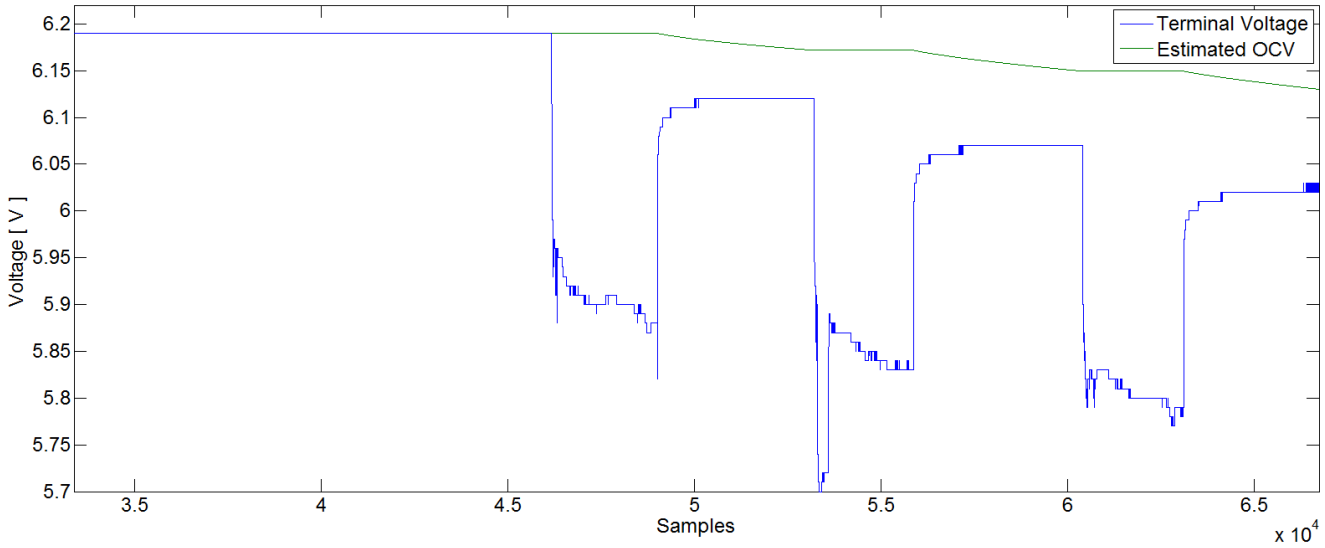

Calculated OCV and terminal voltage after the first reset of the method

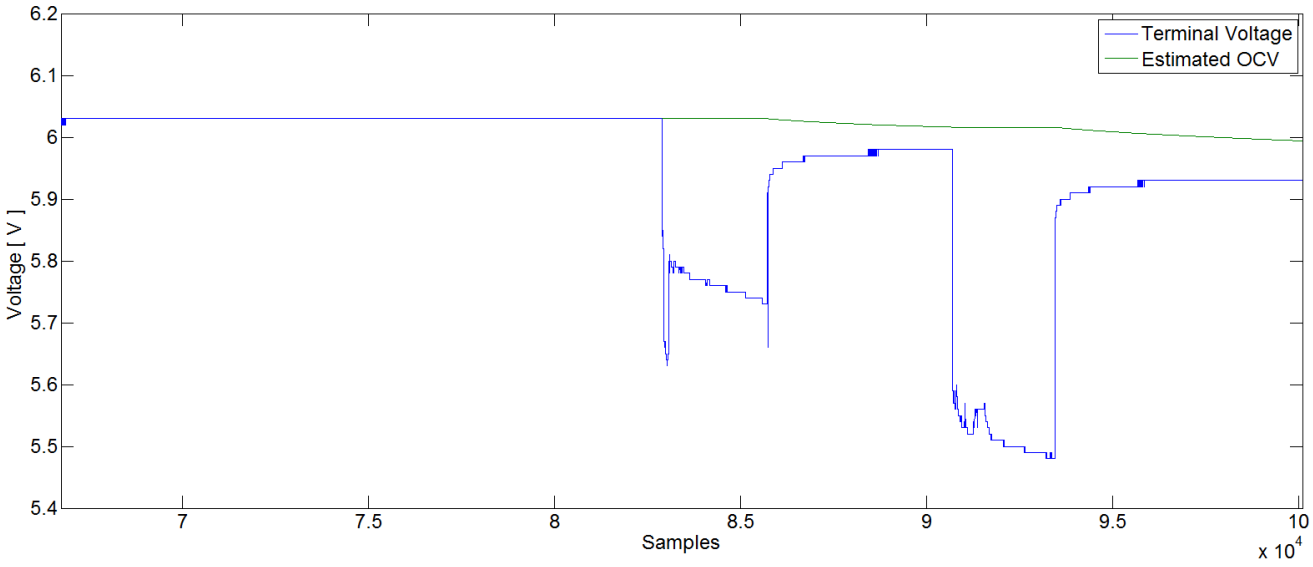

Fig. 4.1.6 Calculated OCV and terminal voltage after the second reset of the method

It is observed that resetting the algorithm significantly improves the precision of OCV calculation. However, the error between the terminal voltage value reaching real OCV and the calculated one in figure 4.1.5 is equal to around 0.1 V which still indicates a low precision of the estimate. The big disadvantage of the presented method at its current state is the necessity to manually choose the reset times of the method.

In order to calculate SOC based on the estimated value of OCV a curve is to be used which was presented in the figure 3.5.6 in the section 3.5.2 of this paper. Calculated SOC is presented in figure 4.1.7:

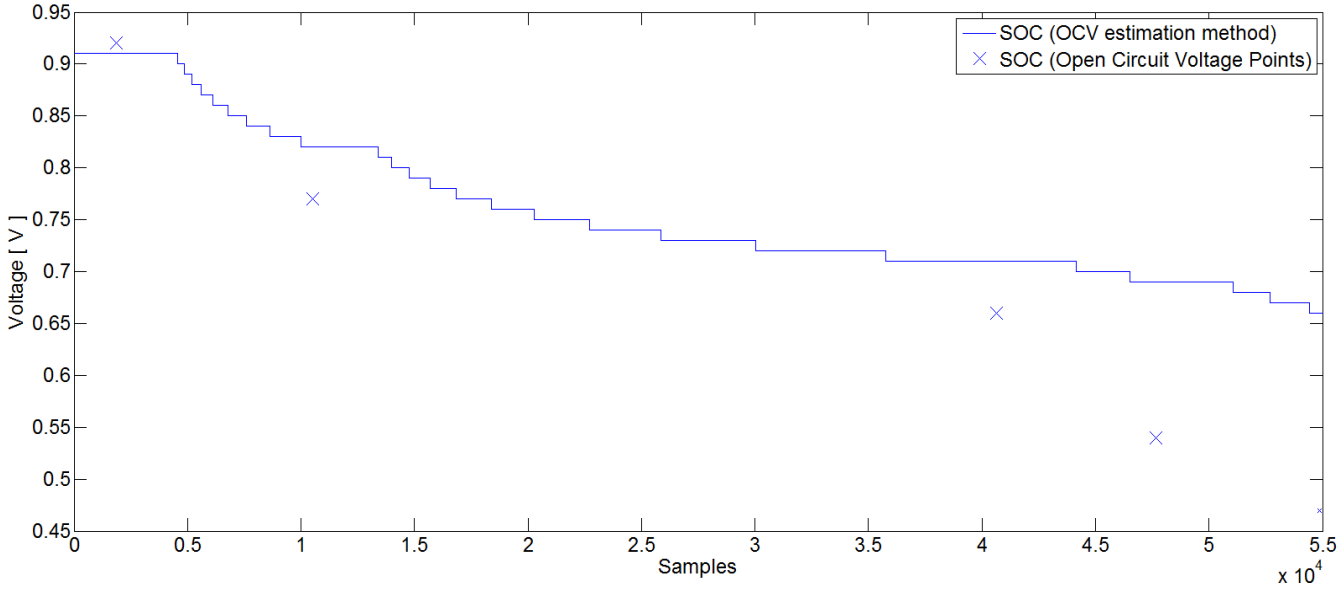

Fig. 4.1.7 SOC calculated by the reference method

In the presented figure, the values real SOC values are denoted by the 'x' signs. Those points were derived from the real OCV (the voltage values which are not changing for at least 2700 samples when the battery is put on hold). The curve was cut off after 55000 samples as the error between the calculated and real SOC became too high. It is imperative to state once again that the method requires resetting in order to work properly. Obtained results might differ from those achieved in the paper wrote by John Chiasson. However, those presented in the aforementioned paper show that the method was reset at least two times in the time span of 1000 seconds. It was shown that the method cannot handle calculation of OCV over longer period of time without frequent resets. Presented method could benefit greatly from the correction factor described in the designed method section.

The comparison of the reference method and Coulomb Counting is presented in the figure 4.1.8.

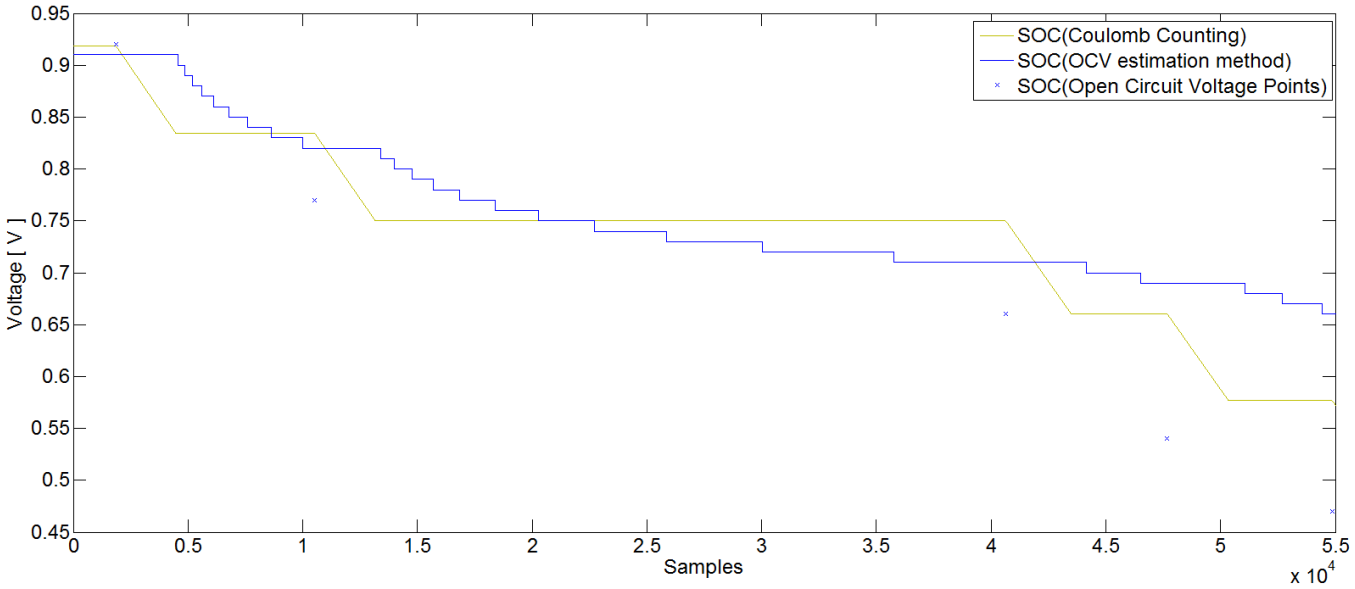

Fig. 4.1.8 Comparison of the reference method and Coulomb Counting

The comparison was done with the Coulomb Counting as both of these methods are used to estimate the OCV when a battery is charging or discharging. The experiment indicates that in the long run (more than 10 hours) both the Coulomb Counting as well as the reference method yield high difference compared to measured open circuit voltage points. I.e. more than 0.1 volt which corresponds to more than 10% difference in SOC. In the shorter time perspective (less than 10 hours) the difference for the comparison estimation method is less than 5% and the Coulomb Countng less than 10%.

The comparison method experiment indicate that the estimation method improve Coulomb Counting and seems to be close to fulfilling Micropower's requirements.

4.2. Designed Algorithm

Both comparison and the coulomb counting methods could be improved by the use of periods when no current is drawn, however it has been chosen to show the improvement of the coulomb counting as it is more widely used in the industry and already implemented in a Micropower measurement tool.

In this part of the chapter, precision of designed algorithm will be evaluated on a sample measured current (Figure 4.1.1) and voltage (Figure 4.1.2) graphs as inputs. To keep the consistence all the graphs presenting different variables from chapter 3, "Implementation" were derived using the same voltage and current graphs.

The graph showing the changes in SOC based on regular coulomb counting and the desired SOC based on OCV is presented in the figure 4.2.1.

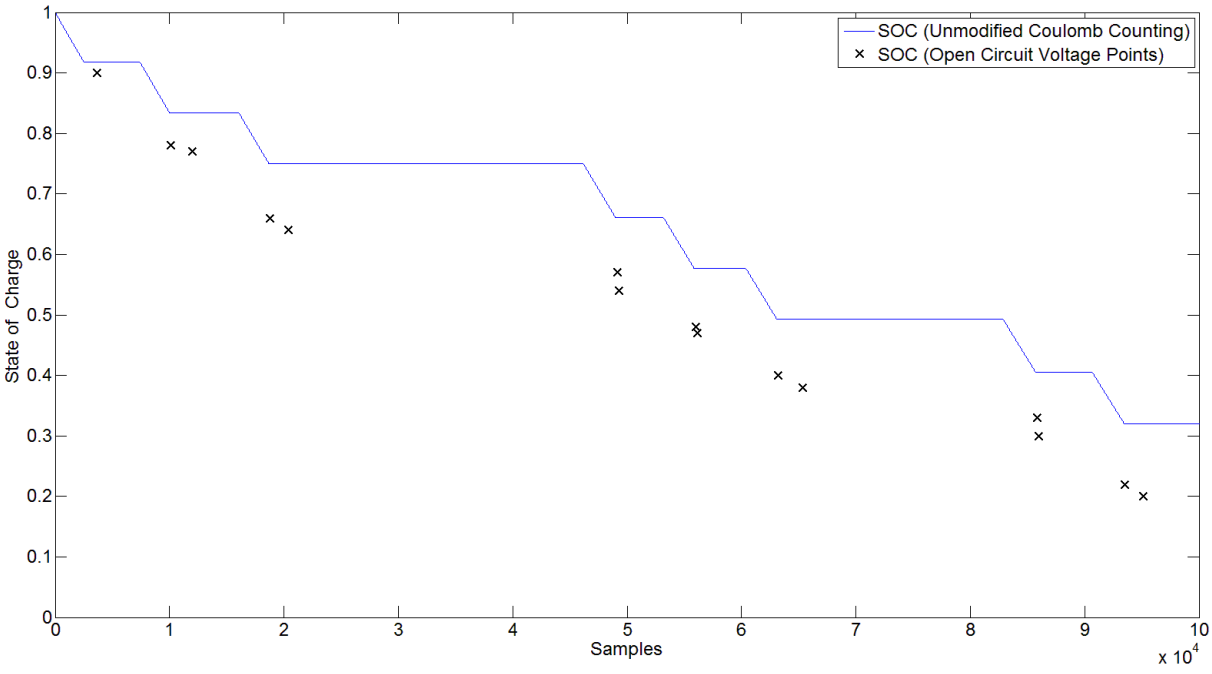

Fig. 4.2.1 Unmodified Coulomb Counting SOC compared to SOC based on OCV

The original Coulomb Counting generates an unacceptable error in most of the points when OCV can be measured or estimated. The differences between both SOC measurements observed in the figure 4.2.1 show the reason why there was a need to implement the algorithm described in this Thesis. Without a feedback, the original, unmodified coulomb counting blindly integrates the measured current values. Not only this procedure is very dependent on the sampling time and a data collection device, but also progressively adds the variable measurement error. The error varies between 2% and 12% during the simulation. For the following reasons it is rather unpredictable algorithm, which needs improvement.

The results of algorithm improvement, presented as changes in SOC based on the improved coulomb counting along with the desired SOC, based on OCV are presented in the figure 4.2.2.

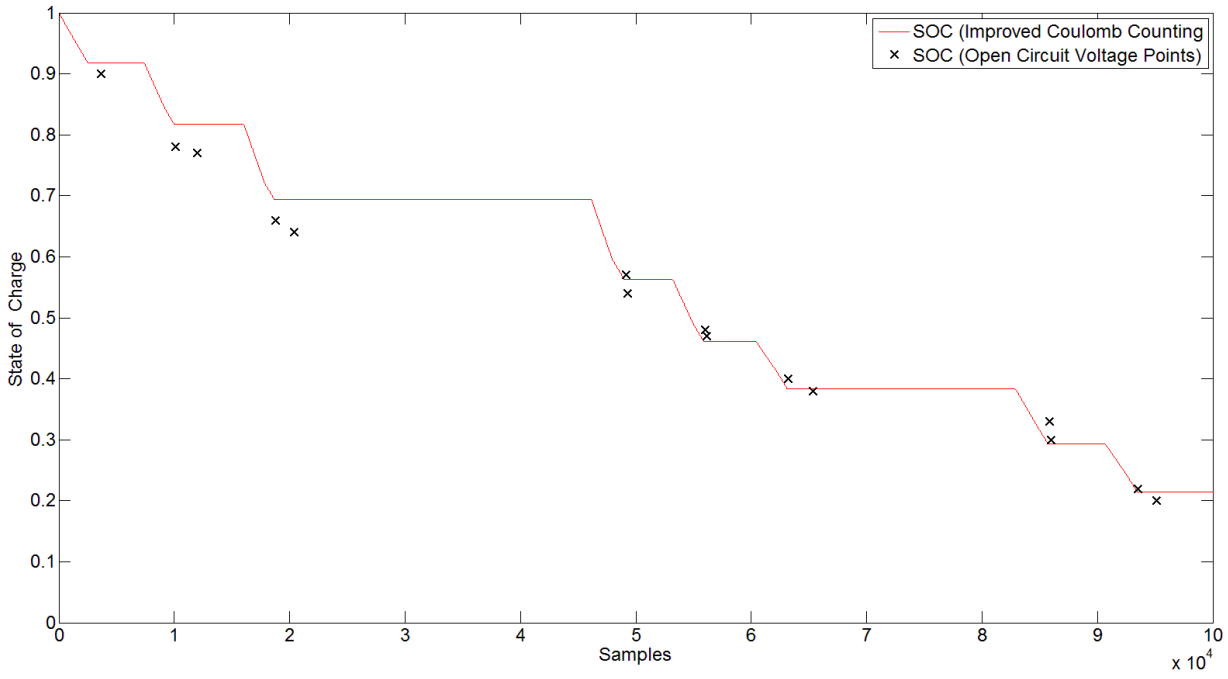

Fig. 4.2.2 Improved Coulomb Counting SOC compared to SOC based on OCV

According to the regressive corrections foundation of the algorithm, the error seen as a difference between the red line and the black crosses on the chart is greater at start and reduced with the further discharge periods. It is conspicuous that the SOC values obtained with use of the designed improved coulomb counting algorithm are much closer to the desired SOC/OCV points. The error values in all highlighted moments vary between 1 and 5% and are reduced over time. With the exception when the OCV estimate does not manage to reach the real OCV value, produces increased error, but corrects itself within next 100 samples. The

charts presented in the figure 4.2.1 and 4.2.2 were combined and pictured as the figure 4.2.3 to simplify the methods' comparison.

Fig. 4.2.3 Comparison of both regular and improved coulomb counting methods

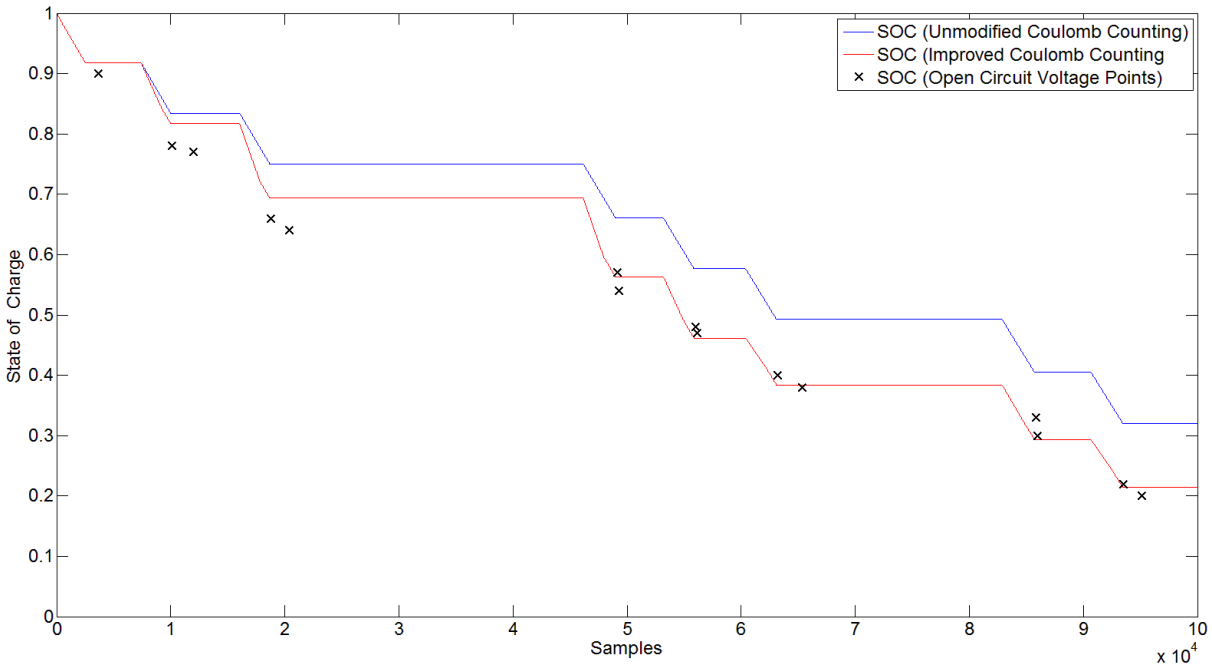

Table 4.2.1 contains error between each chart and the desired value in the highlighted sample values (in which the OCV value has changed - was measured or estimated).

Real SOC	Coulomb Counting	Improved Coulomb Counting
89%	0,02	0,02
78%	0,05	0,04
77%	0,06	0,05
65%	0,09	0,03
64%	0,11	0,05
56%	0,09	-0,01
54%	0,12	0,02
47%	0,10	-0,02
46%	0,11	-0,01
38%	0,09	-0,02
36%	0,11	0,00
32%	0,07	-0,04
30%	0,10	-0,01
21%	0,10	-0,01
20%	0,12	0,01

Tab. 4.2.1 Error values in certain SOC points.

According to the table 4.2.1, the designed algorithm produces reasonably low error values during the whole discharge period, providing the forklift operator with a dependable estimate of the battery state of charge in any time of the discharge.

5. Conclusions and future work

5.1. Conclusions

The purpose of the presented thesis was to design an SOC estimation algorithm which would fulfill requirements presented in the section 3.1. All of the mentioned requirements were met with certain limitations. Firstly, the SOC error is below 5% which was shown in the table 4.2.1. However, unless the changes proposed in section 3.5.3 are implemented, precision level will decrease with the battery aging. No parameterization is required for the algorithm to start, however, its precision is highly dependent on the frequency of the discharge breaks' occurrence. All of the available measured variables are used. The only manual input required from the operator is the nominal capacity of the battery in the beginning of algorithm operation. Although the algorithm is implemented in MatLab SimuLink environment, it may be easily transitioned into C programming language.

The results of the reference method presented in the thesis justifies the use of black-box approach in the algorithm's design. The method created by John Chiasson and Baskar Vairamohan was implemented with consideration of the aforementioned requirements. The comparison method in the time interval less than 10 hours almost fulfills the requirement of 5% maximum error. Higher precision could be achieved with addition of proper parameterization, optimization and resetting of the algorithm. However, the purpose of the Thesis was to design an algorithm with the minimum input from the operator which excludes the reference method. Presented results confirm that for the specific purpose specified in this thesis, black-box modeling yields better results.

5.2. Future work

Even though all the primary objectives were achieved there is still plenty of room for improvement. The main weakness of the Improved Coulomb Counting algorithm is undoubtedly the need of the discharge breaks during its work, as only then the error value can be counted. Naturally, without error value, the correction factor cannot be counted and the flat coulomb counting may not be evaluated. In recent state the algorithm is aimed exclusively at HEVs and EVs, which typically have several breaks during their operation cycle. The idea of using so called "Current Profiles" is a way to extend the algorithm's applications and broaden its functionality.

In shortage: the current profiles would exclude the necessity of breaks in the battery discharge, by saving the information regarding the previous:

- discharge period lengths
- average current values throughout the discharge periods
- the error produced in those periods

Saved as a vector, ex. [200, 14, 0,02] ([samples, Amperes, error value]) the information might be stored (forming a database), corrected over time and used if there is a constant discharge for at least two hours. Such solution would exclude the need of stopping the discharge during the operation cycle, extending the algorithm applications into many different regions.

The current profiles idea was discussed and seriously taken into consideration, but in the end it was not implemented in this thesis. However the solution is advised to be implemented as soon as there is a need for using the algorithm in any other applications than mentioned in this thesis as this could be done by identifying an exponential function for the OCV recovery and stored as just a couple of parameters.

s

6. References

1. K. M. Abraham, Z. Jiang, ”A polymer Eelctrolyte-Based Rechargeable Lithium/Oxygen Battery”, Journal of the Electrochemical Society, Vol. 143, 1996

2. Matthew Barth, Jie Dy, Jay Farell, Shuo Pang, ”Battery state-of-charge estimation”, Proceedings of the American Control Conference, Vol. 2, June 2001

3. Massimo Ceraolo, “New Dynamical Models of Lead-Acid Baatteries”, IEEE Transactions On Power Systems, Vol. 15, NO. 4, November 2000

4. D. Sutanto, H.L. Chan, “ A New Battery Model for use with Battery Energy Storage Systems and Electric Vehicles Power Systems”, Power Engineering Society Winter Meeting, January 2000

5. John Chiasson, Baskar Variamohan, “Estimating the State of Charge of a Battery”, Transactions on Control Systems Technology, Vol. 13, NO. 3, May 2005

6. D.Jaya Deepti, V. Ramanarayanan, “State of Charge of Lead Acid Battery”, Proceedings of India International Conference on Power Electronics, 2006

7. Francisco M. González-Longatt, “Circuit Based Battery Models: A Review”, 2DO Congreso Iberoamericano De Estudiantes De IngenierÍa Eléctrica, 2006

8. James A Gucinski, David F Smith, ”Synthetic silver oxide and mercury-free zinc electrode for silver-zinc reserve batteries”, Journal of Power Sources, Vol. 80, July 1999

9. Yao-Feng Huang, Chin-Sien Moo, Kong-Soon Ng, Yao-Ching Hsieh, ”An Enhanced Coulomb Counting Method for Estimating State-of-Charge and State-of-Health of Lead-Acid Batteries”, Hsieh INTELEC 2009 -31st International Telecommunications Energy Conference, 2009

10. Robyn A. Jackey, ”A simple, Effective Lead-Acid Battery Modeling Process for Electrical System Component Selection”, SAE Paper, 2007

11. Hurng-Liahng Jou, Jinn-Chang Wu, Yu-Hua Sun, “Aging Estimation Method for Lead-Acid Battery”, IEEE Transactions On Energy Conversion, Vol. 26, NO. 1, March 2011\

12. H.A. Kiehne, “Battery Technology Handbook, Second Edition”, Taylor & Francis Group, August 2003

13. Dirk Uwe Sauer, Heinz Wenzl, “ Comparison of different approaches for lifetime prediction of electrochemical systems-Using lead-acid batteries as example”, Journal of Power Sources, Vol. 176, NO. 2, February 2008

14. http://www.batterycouncil.org

15. Fullriver battery company, “Performance Characteristics – DC Series Batteries”: http://www.fullriverdcbattery.com/media/pdf/technical/performance_characteristics.pdf

16. Barrie Lawson, “State of Charge (SOC) Determination”, Woodbank Communications, Electropaedia: http://www.mpoweruk.com/soc.htm

17. Trojan Battery Company, “Comparing deep-cycle flooded batteries to VRLA Batteries”, http://www.trojanbatteryre.com/Tech_Support/ComparingFlood2VRLA.html

18. A project of Battery Council International, Lead-Acid Battery info, ”Lead-Acid battery uses”: http://www.leadacidbatteryinfo.org/lead-acid-battery-uses.htm

19. Battery University – How to measure state of charge http://batteryuniversity.com/learn/article/how_to_measure_state_of_charge